ACS APPLIED MATERIALS & INTERFACES

Review

www.acsami.org

Oligothiophene Semiconductors: Synthesis, Characterization, and Applications for Organic Devices

Lei Zhang,[†] Nicholas S. Colella,[†] Benjamin P. Cherniawski,[†] Stefan C. B. Mannsfeld,[‡] and Alejandro L. Briseno*[,†]

[†]Department of Polymer Science and Engineering, Conte Polymer Research Center, University of Massachusetts, 120 Governors Drive, Amherst, Massachusetts 01003, United States

[‡]Stanford Synchrotron Radiation Lightsource, Menlo Park, California 94025, United States

ABSTRACT: Oligothiophenes provide a highly controlled and adaptable platform to explore various synthetic, morphologic, and electronic relationships in organic semiconductor systems. These short-chain systems serve as models for establishing valuable structure−property relationships to their polymer analogs. In contrast to their polymer counterparts, oligothiophenes afford high-purity and well-defined materials that can be easily modified with a variety of functional groups. Recent work by a number of research groups has revealed functionalized oligothiophenes to be the up-and-coming generation of advanced materials for organic electronic devices. In this review, we discuss the synthesis and characterization of linear oligothiophenes with a focus on applications in organic field effect transistors and organic photovoltaics. We will highlight key structural parameters, such as crystal packing, intermolecular interactions, polymorphism, and energy levels, which in turn define the device performance.

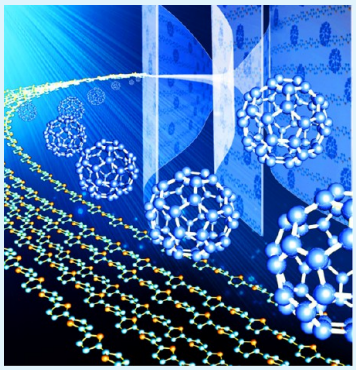

KEYWORDS: *oligothiophenes, crystal packing, organic device, intermolecular interactions, polymorphism*

1. INTRODUCTION

Polythiophenes are among the most highly investigated semiconductor materials for applications in organic electronics because of their efficient charge transport properties, low cost, and compatibility with flexible substrates.[1−4] It has become clear in recent years that structural order in these materials improves the properties, such as charge transport, that lead to better performance in devices. Therefore, any information regarding the self-assembly of these molecules in the solid state is important and valuable.[5−11] However, to understand the optical and electronic properties of semiconductor polymers, one must study well-defined systems.[12] This is not a trivial problem for polymer-based systems, as batch-to-batch variation in molecular structure, including head-to-tail coupling and chain length, and sensitivity to processing conditions can drastically alter the performance characteristics of these materials.[13−16] The experimental conditions must be painstakingly optimized to produce reliable, compelling data. Although this trial-and-error approach has proven fruitful, resulting in organic photovoltaics with efficiencies beyond 8%[17,18] and organic thin film transistors exhibiting mobilities of over 1 cm^2 V^{-1} s^{-1},[19−23] it does not address the true maximum potential of these materials.

Oligothiophenes with the same repeat unit structure as their polymer counterparts offer the opportunity to study the true charge transport nature of these materials, free from structural defects.[24−33] The absence of chain entanglement allows these molecules to form crystals suitable for X-ray single-crystal analysis. This reveals detailed information on the chain packing in the solid state, which plays an important role on the device performance. Furthermore, the syntheses of oligomers can be well-controlled, resulting in monodisperse populations. These well-controlled systems have been widely used as semiconductors in organic devices. Power conversion efficiency (PCE) of 6.9% and mobility up to 6 cm^2 V^{-1} s^{-1} have been achieved based on functionalized oligothiophenes.[34,35] A number of comprehensive reviews of the oligothiophenes and their applications have been published over the past few years.[24,36−38] In this review, we will describe the recent progress in the synthesis oligothiophenes and their applications in organic transistors and organic solar cells. In particular, we will highlight the parameters which play important roles in device performance, such as crystal packing in the solid state, polymorphism, intermolecular interactions, and conjugation length as well as discuss the X-ray techniques used to characterize oligomer thin films.

2. SYNTHESIS OF OLIGOTHIOPHENES

The past decade provided a variety of methods to synthesize polythiophenes and their derivatives.[39] Many of the modern oligothiophene syntheses are borrowed and adapted from these methods. However, most of them provide methods for the synthesis of short oligothiophenes (less than 8 units).[40,41] Fortunately, the recent success in the exploration of the

Received: December 30, 2013
Accepted: March 18, 2014
Published: March 18, 2014

   dx.doi.org/10.1021/am4060468 | ACS Appl. Mater. Interfaces 2014, 6, 5327−5343

Scheme 1. Strategic Routes for the Synthesis of Long Oligothiophenes: (A) Oxidative Coupling, (B) Palladium-Catalyzed C−H Homocoupling, and (C) Palladium-Catalyzed Cross-Coupling

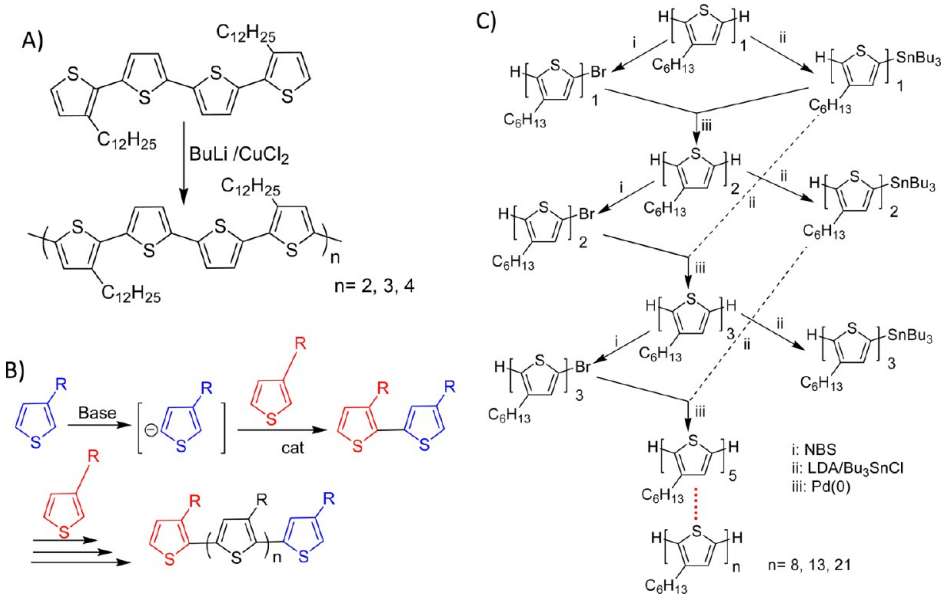

effective catalysts and the development of versatile building blocks have resulted in a wide variety of defect-free, monodisperse, long oligothiophenes.

2.1. Oxidative Coupling. Thiophene derivatives can be either oxidized in the presence of certain oxidizing agents, such as ferric chloride, or deprotonated and then dimerized by $CuCl_2$ to form a mixture of short α-conjugated oligomers (Scheme 1A).[42,43] This method takes advantage of the varying electron density at different positions of the thiophene monomer; the coupling mainly occurs at the positions of the highest electron density.[44] Although this method is very simple, it became rapidly evident that the oligomers produced by this method contain considerable amounts of undesirable $\alpha-\beta$ couplings and regioirregularity, both of which have a detrimental impact on the conjugation and crystallinity of the polymers.[45] It should also be noted that an increase of conjugation in the precursor molecule causes a rapid loss of reactivity of the corresponding cation radical, resulting in short oligomers.[42]

Another major problem with this technique is the purification of the materials. Repeated sublimation and tedious chromatographic separation are needed to purify the desired product because of metal residues that often contaminate the desired products. Recently, Bäuerle and coworkers described a new "metal template approach" to synthesize oligothiophenes. The preparation of the oligothiophenes involves a reaction between lithiated shorter oligothiophenes and $dppfPtCl_2$ or $dpppPtCl_2$ to afford an oliothiophene-based Pt complex, which was then oxidized to the longer oligothiophenes by treatment with silver triflate.[46]

2.2. Palladium-Catalyzed C−H Homocoupling. Transition metal-catalyzed cross-coupling has been well explored for the synthesis of polythiophenes.[39] It has been proven that these reactions proceed by a chain growth mechanism and therefore it is difficult to synthesize monodisperse oligomers with precise molecular weight. Mori and coworkers developed a new synthetic strategy involving the palladium-catalyzed C−H homocoupling of bromothiophene in the presence of a silver reagent system as an activator.[47,48] This technique results in oligothiophenes with C−Br bonds at the terminal rings, which can be further functionalized. More recently, these authors reported an improved procedure for the synthesis of HT oligothiophenes. Treatment of 3-alkylthiophene with Knochel−Hauser base (TMPMgCl·LiCl) induces metalation at the 5-position selectively. Subsequent addition of 2-bromo-3-alkylthiophene and a nickel catalyst leads to the corresponding bithiophene (Scheme 1B).[49] The obtained bithiophene is converted to the terthiophene and then to the quaterthiophene by repeating an analogous protocol.

2.3. Palladium-Catalyzed Cross-Coupling. This synthetic strategy relies on the divergent−convergent approach to conjugated oligomers, which affords monodisperse molecular systems with relatively facile isolation and purification. Typically, long oligothiophenes are prepared by the successive addition of bromine, tin, and/or boronic acid groups to thiophene intermediates for palladium catalyzed cross-coupling, such as Stille or Suzuki reactions.[24,41] Recently, Briseno and coworkers prepared a series of didodecyl-quaterthiophene oligomers with up to 24 thiophene units via Pd-catalyzed Stille coupling reactions.[50] In recent papers, regioregular head-to-head oligothiophenes have been efficiently prepared by combining Pd-catalyzed Stille coupling reactions with microwave radiation.[51] Heeney and coworkers also reported the synthesis of regioregular oligo (3-hexylthiophene) up to a length of 36 units with large quantities via "Fibonacci's route" (Scheme 1C).[52] To get longer homologues, oligothiophenes need to be selectively functionalized at the terminal α-positions. However, the reactivity at α-positions of long oligothiophenes decreases and the possibility of reaction at ß-positions increases due to the increase of the number of ß-positions relative to α-positions with increased chain length.[53] This presents a major problem, as the desired α-linked products are inseparable from the undesirable ß-linked products. To avoid the undesirable ß-reactions, the use of substitutent groups to block the ß-positions is a possible solution. Otsubo and coworkers designed a complete ß−blocked monomer which allowed for the formation of extraordinarily long oligothiophenes, up to 96 units, by the combination of oxidative coupling and cross-

dx.doi.org/10.1021/am4060468 | ACS Appl. Mater. Interfaces 2014, 6, 5327−5343

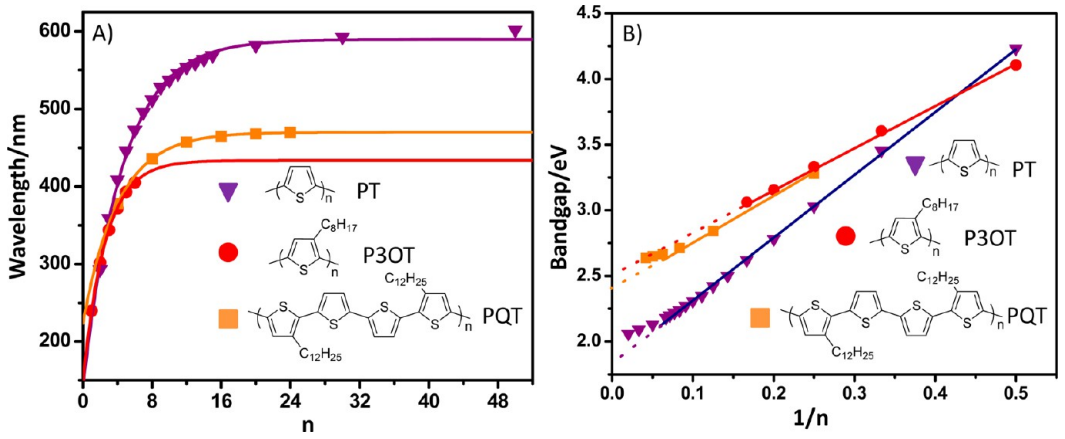

Figure 1. (A) Correlation between the maximum absorption (λ_{max}) and ring numbers (n) of oligothiophenes, and (B) bandgap energy vs inverse ring number.

coupling reactions.[28] Although this route requires a number of synthetic steps, it simplifies the purification significantly.

3. DETERMINING CONJUGATION LENGTH IN OLIGOTHIOPHENES

On a molecular scale, the optoelectronic properties in semiconductor systems are largely a result of the degree of conjugation. The conjugation and the resulting band gap in solution are restricted by four variables: variation in bond length (known as Peierls distortion), torsion along the polymer backbone, aromatic resonance, and electronic effects from side groups.[44] These factors limit the delocalization of orbitals and lead to the oligomer exhibiting an effective conjugation length, n_{ecl}. Thus, an oligomer of length equal to or greater than the n_{ecl} is electronically commensurate with the polymer.

The highest occupied molecular orbital (HOMO) and the lowest occupied molecular orbital (LUMO) levels, as well as the resulting band gap, are direct results of electron delocalization within a molecule. As such, there is a clear inverse relationship between the band gap and the number of monomers, i.e. the absorption of longer oligomers is red-shifted. According to classic Kuhn theory, this can be modeled as

$$E_g(N) = V_0 + \left(\frac{h^2}{4mL_0^2} - \frac{V_0}{4}\right)\frac{1}{N + 0.5}$$

where h is Planck's constant, m is the mass of an electron, L_0 is the average length of a conjugated bond, and V_0 corrects for Peierls distortion.[54] However, this underestimates the band gap of the polymer and a clear deviation from linearity is observed for high molecular weight oligomers. A more accurate model was put forth by Meier which divides the band gap into two components.[55] The first component is representative of the band gap of an infinitely long polymer and the second component accounts for effect of conjugation going from the monomer to polymer, with an exponential decay.

$$E_g(n) = E_g(\infty) + (E_g(1) - E_g(\infty))e^{-a(n-1)}$$

$$\lambda(n) = \lambda(\infty) - (\lambda(\infty) - \lambda(1))e^{-b(n-1)}$$

where n is the number of repeat units, $E_g(1)$ and $E_g(\infty)$ are the band gaps of the monomer and infinite polymer, respectively, $\lambda(1)$ and $\lambda(\infty)$ are their corresponding wavelengths, and a and b are the rates of convergence. By fitting experimental UV−vis data to this model, one can determine the effective conjugation length where the absorption is within 1 nm of the infinitely long polymer.

$$n_{ecl} = \frac{\ln(\lambda(\infty) - \lambda(1))}{b} + 1$$

Bendikov and coworkers compared a number of density functional theory (DFT) quantum mechanical modeling methods to calculate the energy levels of a series of oligomers.[56] They found that the $1/n$ Kuhn approximation overestimated the absorption of the polymer and did not account for the limitations of conjugation when $n > 12$ for any models. Additionally, they concluded that although the HF/6-31G(d) and BLYP/6-31G(d) levels of modeling converged, they did not accurately predict the optoelectronic structure for unsubstituted polythiophenes, yielding band gaps of 7.43 and 0.93 eV, respectively. The B3LYP/6-31G(d) level, especially when incorporating periodic boundary conditions (PBC) in the calculations, accurately modeled the band gap of oligothiophenes when using sufficiently long oligomers (up to $n = 50$). These calculations predicted a band gap of 2.06 for the polymer, which has a band gap of 2.0 when measured experimentally.

Oligo- and polythiophenes typically incorporate alkyl side chains to enhance solubility for processing; these bulky groups induce twisting along the backbone. This out-of-plane deformation limits the electron overlap and leads to a decrease in conjugation, increasing the band gap. Lavarda et al. used molecular dynamics simulation to model the conformation of P3HT and found that the dihedral angle between neighboring thiophene units is expected to be 115° in solution.[57] Experimental data is available for a similar system consisting of poly(3-octylthiophene) (P3OT) oligomers (Figure 1).[58] Fitting the obtained UV−vis data to Meier's model, we find that the twisting in P3OT decreases the effective conjugation length to 14.7 thiophene units (Table 1). Furthermore, the reduction in conjugation reduces the maximum absorption of P3OT by 156 nm relative to the calculations for unsubstituted thiophenes.

To produce solar cells with high efficiencies, one needs to optimize the short-circuit current (J_{sc}), open-circuit voltage (V_{oc}), and fill factor (FF).[36,37] The extended conjugation across planar oligomers increases the HOMO and lowers the energy

dx.doi.org/10.1021/am4060468 | ACS Appl. Mater. Interfaces 2014, 6, 5327−5343

Table 1. Absorption and Effect Conjugation Length (ecl) of Different Polythiophenes[a]

	λ_{max} (nm)			n_{ecl} (units)	
	1/n linear fit	exponential fit	experimental	linear fit	exponential fit
PT (theoretical)	685	590	602	20	27.7
PQT	508	470	471	16	22.4
P3OT	488	434	440	12	14.7

[a]The data of unsubstituted oligothiophenes is from theoretical calculations, see ref 58.

of the LUMO of the molecules, decreasing the bandgap. This leads to increased light absorption which generates more excitons, increasing the J_{sc}. Planar oligomers also generally pack better, enhancing charge transport and increasing the FF. Efforts have been made to synthesize soluble polythiophenes which maintain more planar backbones. One approach has been to incorporate fewer, longer alkyl side-chains, as is the case with 3,3‴-didodecyl-2,2′:5′,2″:5″,2‴-quaterthiophene (DDQT). These oligomers have an effective conjugation length of 22.4 thiophene units with a maximum absorption at 470 nm (Table 1).[50] Another approach has been to reduce the steric interactions between the solubilizing groups of neighboring thiophene units. Otsubo and coworkers used a 2,2-bis(butoxymethyl)-1,3-propanediyl group at both β-sites of each thiophene unit to pull the alkoxy side chains away from each other.[28] This "tying back" of the solubilizing groups induced a more planar conformation of the oligomer backbones, extending the effective conjugation length to 20.9 thiophene units and increasing the maximum absorption to 524 nm.

Bäuerle and coworkers further increased the absorption of planar oligothiophenes, which lacked solubilizing side chains, by utilizing dicyanovinyl (DCV) groups as end-caps.[59] These electron-withdrawing moieties reduced the band gap of the rigid molecules, resulting in a theoretical maximum absorption at 547 nm for the corresponding polymer. The pentamer exhibited a maximum absorption at 530 nm, 17 nm higher than that of an equivalent oligomer that contained butyl side chains.[60] It is interesting to note that these oligomers produced an effective conjugation length of only 11 thiophene units because of the large influence of the end-caps on the electronic structure; increasing the length beyond this point would only serve to decrease the effect of the DCV end groups. Because of electron-accepting cyano groups at both ends, the optical band gap of the oligomers reduced as compared to that of unsubstituted quinquethiophene. Figure 2 shows representative oligothiophenes mentioned in this review.

4. CRYSTAL PACKING IN THE SOLID STATE

4.1. Effect of Substituents on Crystal Packing. Unsubstituted oligothiophenes crystallize in the monoclinic space group and display 2D herringbone arrangement due to strong edge-to-face interactions.[61] Although some high mobilities are reported for 2D layered arrangement, the edge-to-face configuration limits the electronic overlap between π orbitals.[62−65] As a result, higher performance may be achieved in crystal structures which exhibit more "π-stacking" because of the strong electronic coupling.[64]

4.1.1. α-Substituted Oligothiophenes. A number of efforts have been made to tune the crystal packing by modifying the molecular structure of the oligomers under study.[62] The incorporation of substituents along the backbone has a dramatic influence on the crystal packing of the oligothiophenes.[38] However, it is somewhat surprising to see that

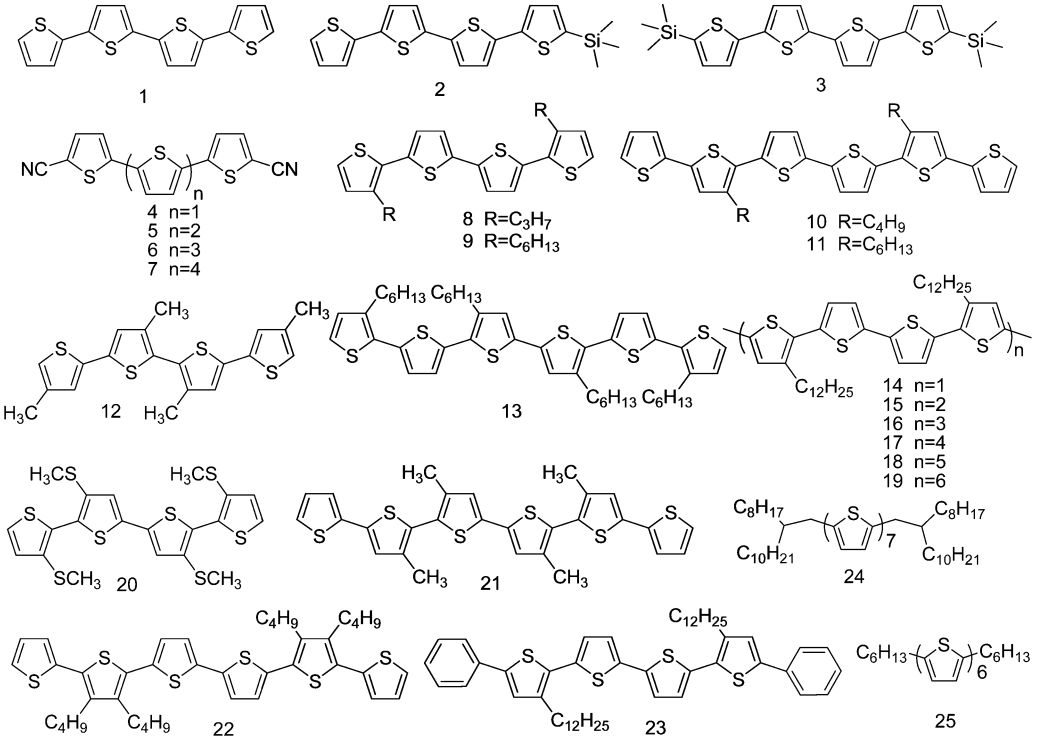

Figure 2. Representative examples of oligothiophenes **1**−**25** in this review.

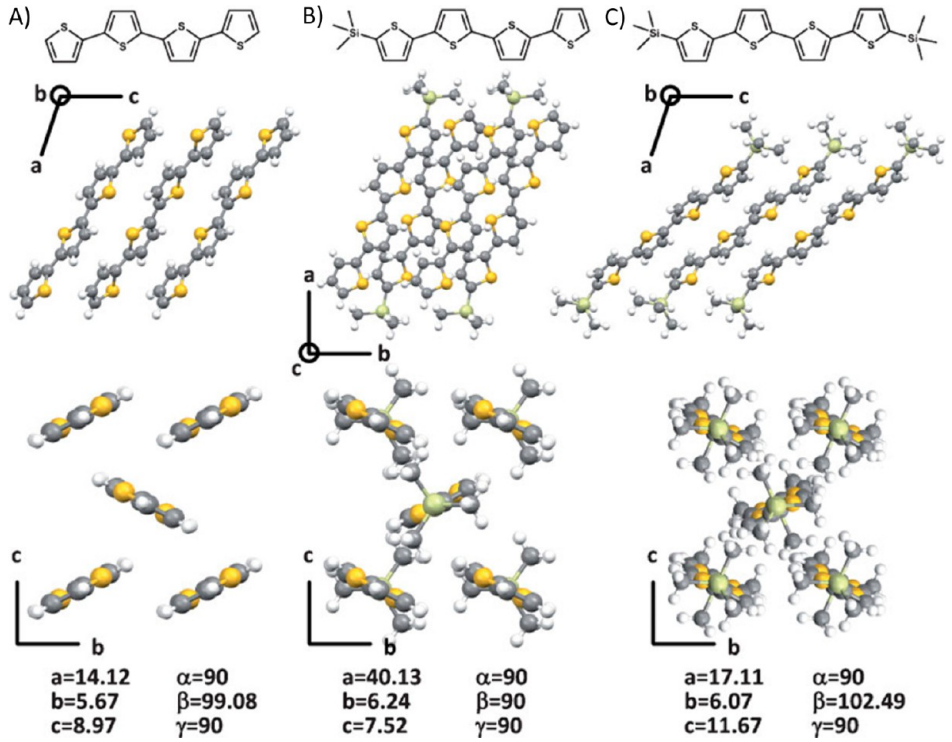

Figure 3. Chemical and crystal structures and lattice parameters of, (A) unsubstituted **1** (high-temperature polymorph), (B) mono-TMS-substituted **2**, and (C) di-TMS-substituted quaterthiophene **3**. Terminal substitution determines the in-plane tilt of the oligothiophene cores, with **3** (51°) > **1** (34°) >**2** (26°). Reprinted with permission from ref 67. Copyright 2009 Wiley.

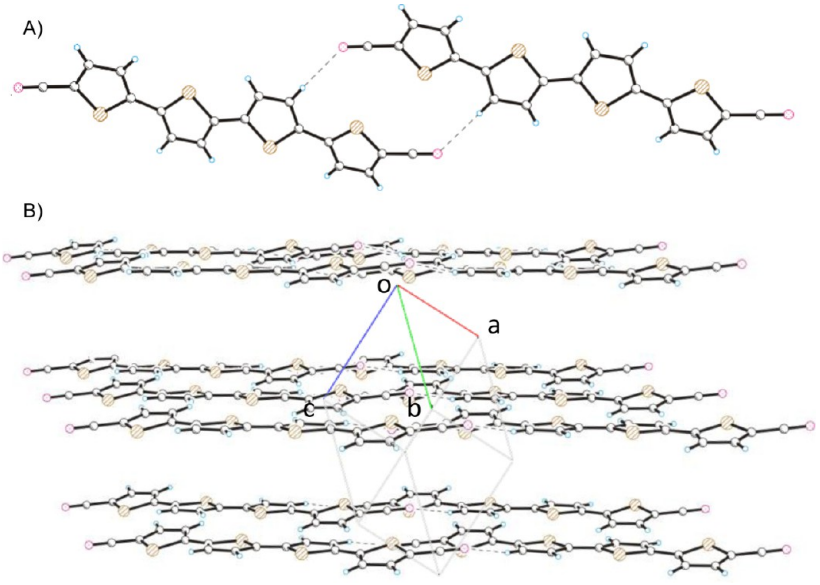

Figure 4. (A) Intermolecular C−N···H interactions, and (B) side view of packing in **5** showing ribbonlike arrays.

substitution at the high electron density (α-) positions with linear alkyl chains or less bulky substituents does not alter the molecular packing motif significantly.[66] As an example, the crystal packing of quaterthiophene terminated with different alkyl chains and different number of trimethylsilyl (TMS) groups has been investigated (Figure 3).[67] It was observed that each of the molecules adopted a layer-by-layer herringbone motif, but the tilt angle of the molecules within the *bc* plane varied with the terminal substitution. This indicates that in addition to enhanced chemical stability and solubility, the end-substitution does not induce inter-ring torsion and the dominant force dictating the crystal packing is the interaction between aromatic cores. Alternatively, branched alkyl chains or other bulky substituents at the α-positions reduce the relative density of the thiophene cores, causing the packing to deviate from the herringbone arrangement.[38]

Barclay *et al.* reported a series of oligothiophenes (**4**–**7**) that were symmetrically substituted by two nitrile groups at the α-positions. Interestingly, in compounds **4**, **5**, and **6**, the intermolecular CN···H interactions linked oligothiophene molecules into extended ribbons, adopting a slipped π-stack motif rather than a herringbone packing (Figure 4).[68] In

dx.doi.org/10.1021/am4060468 | ACS Appl. Mater. Interfaces 2014, 6, 5327−5343

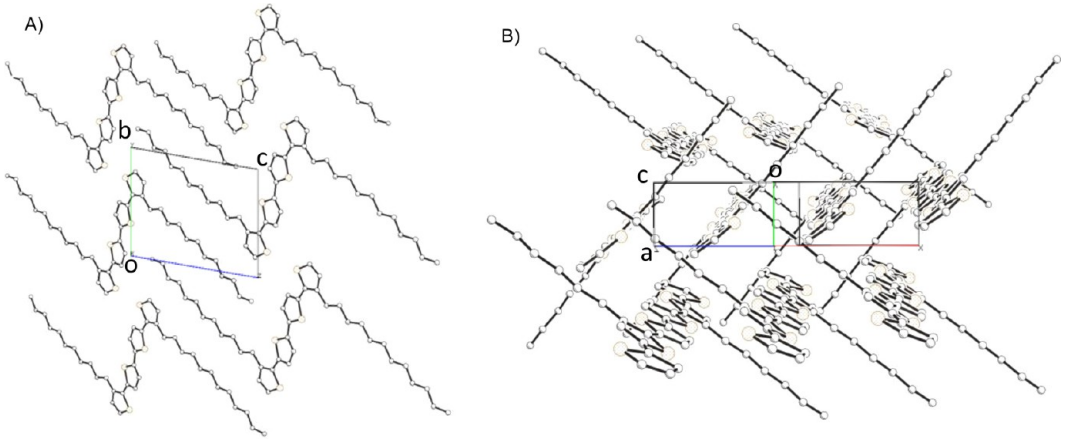

Figure 5. Representative packing models of ß-substituted oligothiophenes. (A) Lamellar packing of **14**, and (B) herringbone packing of **11**.

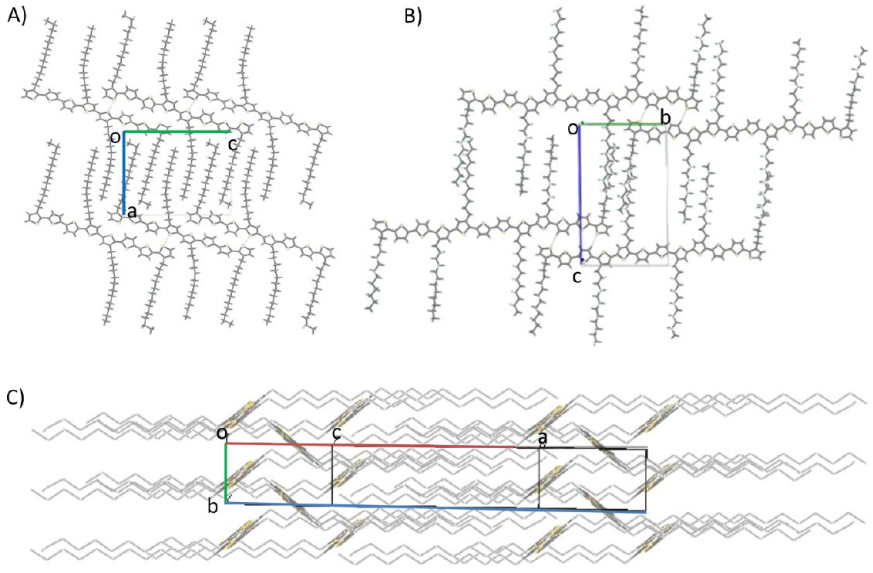

Figure 6. (A) Crystal packing of compound 15 along b-axis; (B) compound 16 along b-axis, and (C) Herringbone packing and alkyl interdigitation of compound 15. Hydrogens were omitted for clarity. Reprinted with permission from ref 50. Copyright 2013 American Chemical Society.

compound **7**, which had the longest backbone of the oligothiophenes in that study, the CN···H interactions were offset to form an interlocking pattern, which allows consecutive molecules along a given ribbon strand to rotate and a herringbone packing pattern to be maintained.

4.1.2. β-Substituted Oligothiophenes. In contrast to substitutions at the α-positions, substitutions at the low-electron-density positions (ß-) have a great effect on the backbone planarity and thiophene conformation.[69] The introduction of a substituent along the backbone may induce a twist along the polymer chain and consequently decrease intermolecular interactions between the thiophene cores.[70,71] This influence is clearly seen in many β-substituted oligothiophenes, which crystallize to form $\pi-\pi$ stacks instead of following the herringbone motif typical of unsubstituted oligothiophenes.[31] The crystal packing behavior of substituted oligothiophenes arises not only from the backbone organization but also from the side chain conformation. The chain length, position, and concentration of substituents all play important roles in the crystal packing.

A family of quaterthiophene derivatives functionalized at the β positions with alkyl chains display differences in the packing depending on the length of alkyl chain.[30] Oligothiophene derivatives with longer alkyl chains, such as **9** and **14**, form lamellar packing motifs by self-assembly through $\pi-\pi$ interactions between cofacial thiophene units and intermolecular dispersive interactions between the alkyl chains which are perpendicular to the backbones (figure 5a). However, a derivative with a shorter alkyl chain, **8**, displays π-stacking which is "slipped" in two directions. The difference in the crystal structures arises from the alkyl side chains: hexyl and dodecyl chains are sufficiently long to provide hydrophobic alkyl−alkyl interactions with neighboring chains, while propyl chains are too short to maintain the hydrophobic interactions between each other.[30] Another interesting example arises when comparing tetramethylquaterthiophene **12**,[72,73] and tetrahexylsexithiophene **13**,[74] which display parallel, layered-type packing in the bulk crystals. It indicates that the ratio of alkyl chains and thiophene units is key to governing the crystal packing characteristics. It is apparent that the compounds with high ratio of alkyl chains to thiophene units potentially exhibit lamellar packing rather than herringbone packing.

It is surprising to see that **10**[75] and **11**[76] show slipped herringbone packing patterns which slightly differ in alkyl chain

dx.doi.org/10.1021/am4060468 | ACS Appl. Mater. Interfaces 2014, 6, 5327−5343

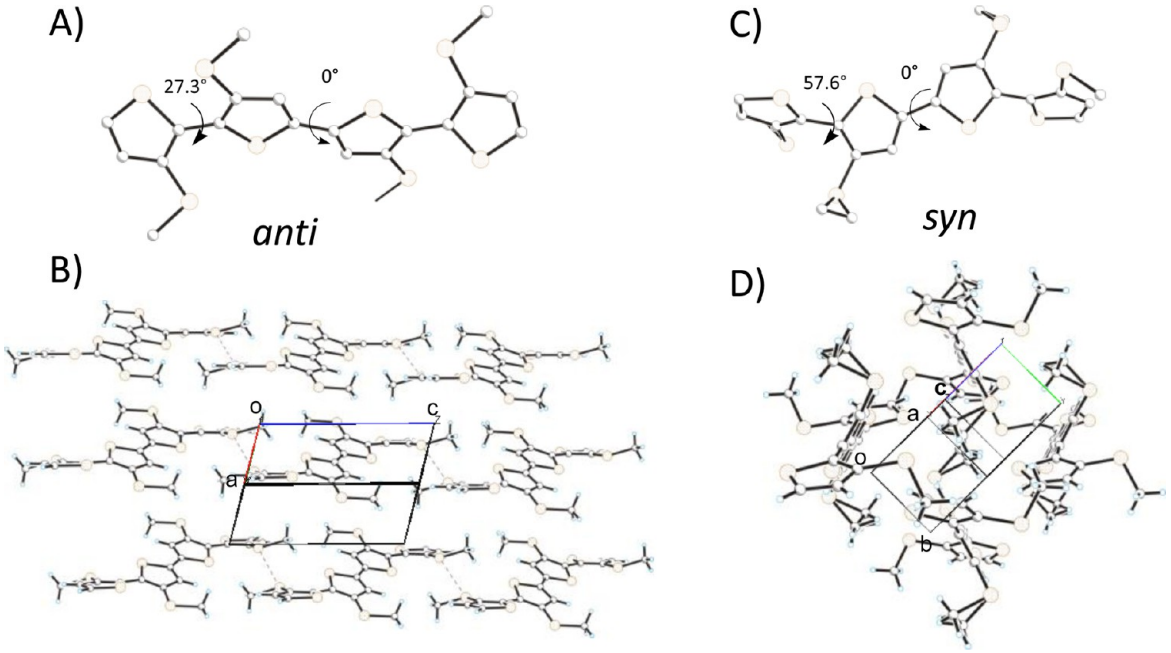

Figure 7. (A, B) Anti-conformation of **20** with triclinic space group and its packing arrangement, (B) crystal structure of **20** with triclinic space group, and (C, D) syn-conformation of **20** with monoclinic space group and its packing arrangement.

orientation (Figure 5b). These structures have a herringbone configuration arranged in layers and separated by the alkyl side chains, with essentially no π-overlap between adjacent molecules. This is likely due to the increased concentration of electrostatic repulsion between cofacial molecules relative to the dispersive interactions of the alkyl side-chains.

The backbone length also has an effect on the crystal packing. Compounds **14** and **16**, a monomer and trimer, respectively, adopt lamellar-type packing motifs by self-assembly through the $\pi-\pi$ interactions of the backbone and intermolecular hydrophobic interaction between alkyl chains (Figure 6).[31,50] However, compound **15**, a dimer, crystallizes in a "lamellar herringbone" packing motif with half of the backbones overlapping. The formation of different crystal packing is possibly due to the difference in symmetry; compound **15** has a lower molecular symmetry with respect to its side chains. It should be noted that the crystal structure of longer oligothiophenes are helpful models for understanding packing trends in corresponding polythiophenes.

4.2. Conformational Polymorphism in the Solid State. It is well-known that because of the weak interaction energies, organic molecules are prone to forming various polymorphs in the solid state.[77] There are some significant differences in the crystal structures, mainly involving molecular packing and intermolecular interactions, which can be greatly affected by substitution patterns, solubility, and crystallization conditions.[78,79]

4.2.1. Backbone Polymorphism. The crystal polymorphism of unsubstituted oligothiophenes has been known for two decades.[80] For instance, there are two different crystal forms of α-4T and α-6T, each of which crystallize in monoclinic space groups. Although both of the two different forms give rise to herringbone packing, a different number of molecules in the unit cell (two and four) and a different tilt angle of the molecular long axis are observed. However, the polymorphism of substituted oligothiophenes arises from not only the backbone conformation, but also the side chain conformation.[80] The thiophene units along the backbone can exhibit anti conformation (the thiophene rings have the sulfur atoms pointing alternatively in opposite directions) and syn conformation (the thiophene rings have the sulfur atoms pointing alternatively in one direction) under different crystallization conditions. The syn-conformations have recently been reported for several oligothiophenes, and theoretical studies indicate that, depending on the substitution pattern of the oligothiophene backbone, the energy difference between syn and anti conformations is rather small.[31]

In compound **20**, which contains methyl sulfide substituents, the molecules crystallize in monoclinic and triclinic space groups. In the triclinic crystal, all of the thiophene rings display an anti conformation to each other, which are illustrated in Figure 7. The torsion angle of the two thiophenes located at the external and internal positions are 27.3 and 0°, respectively.[69,81] This triclinic form has a sandwich-type molecular arrangement instead of the usual herringbone packing. In the monoclinic form, the two terminal thiophenes are in syn conformations with torsion angles as large as 57.6°, resulting in a more twisted backbone. The coplanar inner thiophenes display herringbone packing, while the orientation of the outer rings appears to be mainly determined by intermolecular interactions. Similar polymorphism has been observed in compound **21**, which displays a strongly twisted syn conformation in the monoclinic form, and a less titled anti conformation in triclinic form. The authors attributed this similarity to the fact that substituents on the two molecules have the same regiochemistry.[82]

Compound **22**, a molecule that contains 3,4-disubstituted thiophenes in its backbone, crystallizes in two different forms, each with four molecules in one unit cell. Three of the molecules show all-anti conformations, whereas the fourth exhibit anti conformations except for the two outermost rings, which display *syn* conformations.[70] The thiophene rings adjacent to alkyl groups adopt mainly anti conformations to minimize steric crowding. These results support the idea that the syn or anti conformations are essentially determined by

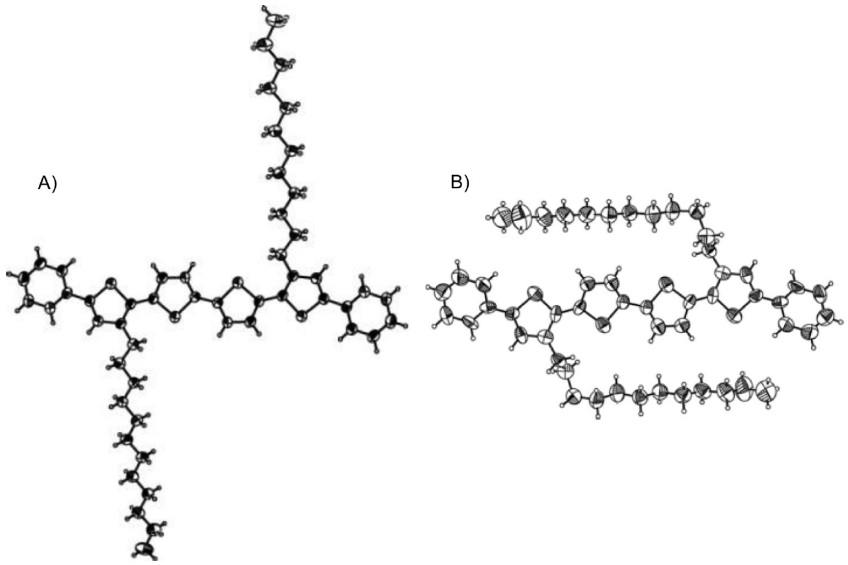

Figure 8. Thermal ellipsoid plots (prepared at the 30% probability level) of single-crystal structures of **23** (A) grown from hexane, and (B) crystals grown from 2-propanol. Reprinted with permission from ref 83. Copyright 2007 Wiley.

packing forces at the detriment of intramolecular forces. It is worth noting that thiophene rings in the *syn* conformation deviate from coplanarity significantly more than those in the all-anti conformation.[31] The steric interactions introduce rotational defects into the backbone, disrupting conjugation. Typically the terminal thiophene rings deviate from coplanarity significantly more than the internal rings, therefore the conjugation length is at least two units shorter than expected.[70] These disruptions may also affect intermolecular charge transport, especially from chain-end to chain-end, decreasing carrier mobility.

4.2.2. Side-Chain Polymorphism. Side-chain conformational arrangement can also affect the polymorphism of oligothiophenes. Such polymorphism has been observed in a family of didodecylquarterthiophenes crystals, depending on the solvent from which they are grown. In non-polar solvents (e.g., hexane, toluene), the molecules crystallize in a herringbone stacking pattern with fully extended dodecyl side-chains which are almost perpendicular to the quarterthiophene backbone.[83] However, in polar solvents (e.g., 2-propanol), the molecules crystallize in a slipped herringbone stacking with bent alkyl chains that are almost parallel to the backbone (Figure 8). The same polymorphism was also observed in the crystalline regions of thin films. From these observations, it is clear that the crystal structure containing bent side chains represents a local energy minimum, whereas the crystals that contain fully extended side chains are more thermodynamically stable.

4.2.3. Thin-Film Polymorphism. It was also found that certain polymorphs only arise in thin films (particularly monolayer films). These "thin-film phases" do not occur in bulk single crystals. Although the crystal structure of thin film polymorphs cannot be resolved by conventional single crystal diffraction methods, the thin films can be characterized successfully by various X-ray diffraction methods and theoretical approach. The appearance of these polymorphs depends on the growth conditions, such as the substrate, temperature, or film thickness.[78,84] For instance, in the monolayers of **24** and **25**, α-functionalized oligothiophenes, the crystal lattice constants are larger compared to those of the several-layer films.[85,86] Recently, Zhe et al. argued that crystallization speed is a key parameter for polymorphism in thin films. Specifically, slow crystallization speed induces preferential growth in the stable bulk structure, while fast crystallization leads to the occurrence of metastable thin-film phases.[87]

4.3. Intermolecular Interactions. Compared to C−H···π interactions, which are commonly found in unsubstituted oligothiophenes and oligo-acenes, there are other types of weak intermolecular interactions in substituted oligothiophenes that can play an important role in determining the crystal packing arrangement.[61,78] For ß-substituted oligothiophenes, in addition to π···π interactions between thiophene rings and dispersive interactions between aliphatic substituents, there are also H···H and C···H interactions between the polymer backbone and alkyl side chains. When the backbone of the oligomer is planar, these interactions can stretch the alkyl chain perpendicularly to the backbone to help to crystallize in parallel, layered-type stacks, especially for oligomers with long alkyl chains.[50] For example, in compounds **9** and **14**, quaterthiophenes with hexyl and didodecyl side chains, respectively, the backbones are locked together by H···H interactions between the thiophene units and alkyl chains to form parallel layers. This phenomenon has also been observed in oligomers with short alkyl chains. In compound **12**, which contains only methyl substituents, the backbone is nearly coplanar with a torsional angle close to 0°.[72,73] The strong interactions between the hydrogen atoms of the methyl groups and the thiophene rings block the edge to face interactions of the herringbone motif.

Another type of molecular interaction widely observed in oligothiophene crystals is the S···S interaction, which can provide enhancement of the electronic dimensionality and provide an alternative charge transport pathway beyond the π···π interactions.[78,88] Additionally, there are multiple intermolecular contacts from S···H, and H···H interactions between overlapped backbones, which have been shown to help stabilize lamellar packing and are favorable for π-electron delocalization and charge transport .[50]

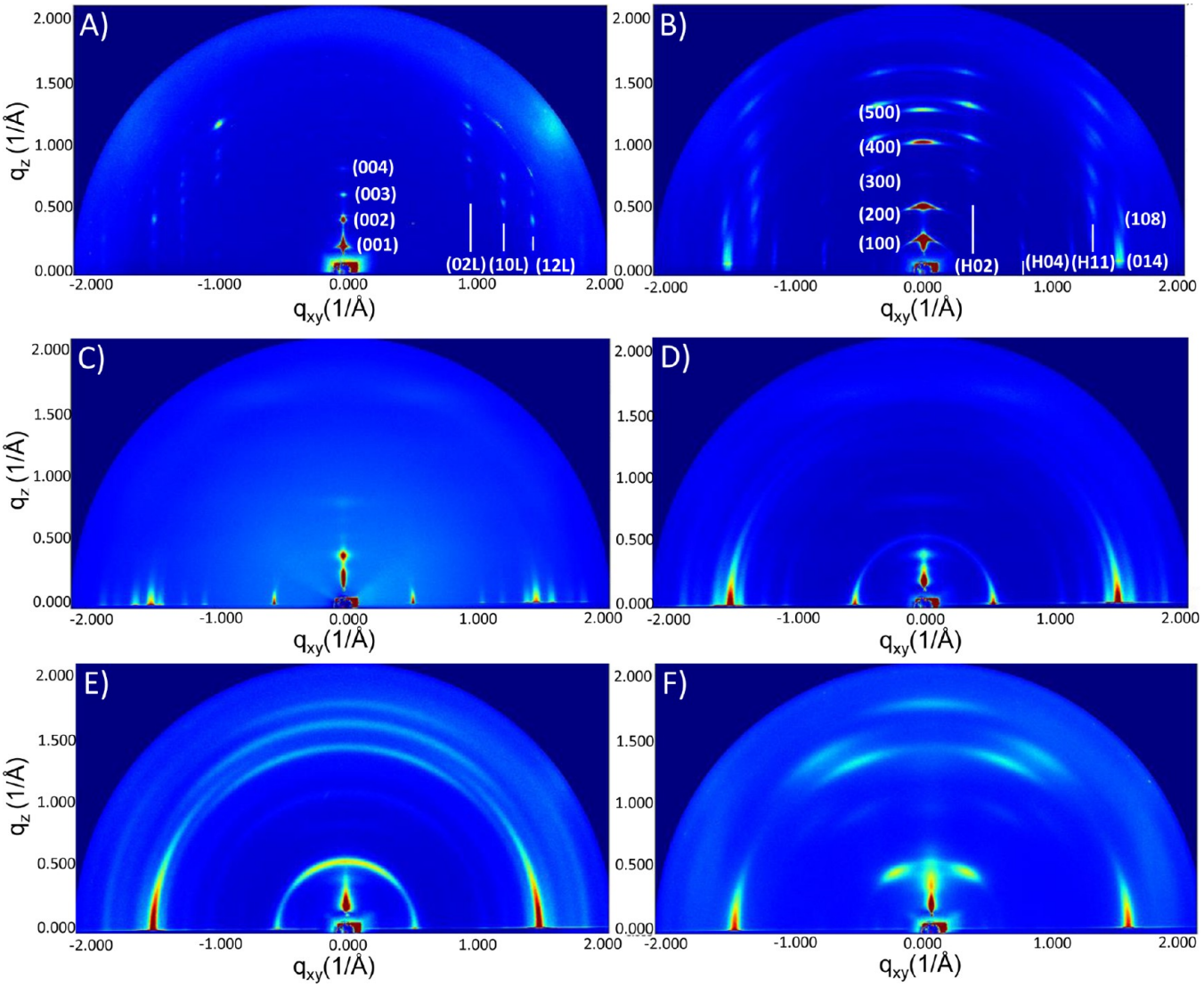

Figure 9. GIXD images of oligothiophenes on Si substrate by spin-cast from chlorobenzene solution. (A) **14**, (B) **15**, (C) **16**, (D) **17**, (E) **18**, and (F) **19**. Reprinted with permission from ref 50. Copyright 2013 American Chemical Society.

5. X-RAY CHARACTERIZATION OF OLIGOMERS

A number of X-ray characterization techniques are suitable to study oligomeric and polymeric thiophene derivatives, such as near edge X-ray absorption fine structure (NEXAFS), grazing incidence X-ray diffraction (GIXD), and polarized soft X-ray scattering (PSoxS). Near edge X-ray absorption fine structure (NEXAFS) has most commonly been employed to study the alignment of the aromatic cores relative to the substrate in crystalline films of oligothiophenes, thiophene-based small semiconductor molecules, and thin films of polythiophenes such as poly(2,5-bis(3-tetradecylthiophen-2-yl)thieno[3,2-b]-thiophene) (PBTTT).[90−93] In those system, the NEXAFS analysis can take advantage of the fact that all dipole moments associated with the electronic 1s-pi* transitions in the carbon atoms forming an aromatic ring system point in the same direction. In the case of planar oligo- or polythiophene ring system, these transistions represent a marker for the orientation of the molecule's aromatic core, and the resonant stimulation of these transitions in NEXAFS experiments, therefore, allows one to estimate the molecular tilt or roll angle relative to the substrate. However, because the NEXAFS signals are averaged over the entire sample, a quantitative analysis of the molecular "tilt angle" based on NEXAFS data heavily relies on a high degree of single-crystalline order or a well-known crystalline texture in the sample. Furthermore, the analysis breaks down for materials with non-primitive unit cells (more than 1 molecule per cell) or when there is significant torsional disorder/twist along the aromatic core. Spectroscopically performed scanning transmission X-ray microscopy (STXM) provides NEXAFS-type orientational information in addition to spatial resolution down to 30−50 nm length scales and was recently applied to oligothiophene thin films.[94]

Hard X-ray diffraction in grazing incidence geometry (GIXD) is the most direct method to analyze the crystalline fraction in oligothiophene thin films and has been used to study oligothiophene films since the earliest days of their use for in organic field effect transistors (OFETs).[95] The position of peaks is directly related to the periodic distances in the thin film and yields the crystalline unit cell. The peak shape on the other hand can contain information on the orientation distribution, the dimensions of the film's crystalline grains, whereas the width evolution of the in-plane peaks at the same position near 1.0 $Å^{-1}$ with increasing scattering vector can be used to quantify

defect density, and paracrystalline disorder in the film. The grain distribution and texture in thin films of oligothiophenes based on DDQT was recently studied by Zhang et al.[50] The diffraction peak shape characteristics in these films vary with the DDQT backbone length, and the evolution from small molecule-like packing to polymer-like packing in DDQT thin films can be followed in the respective GIXD diffractograms (Figure 9). Ong and coworkers directly determined polymorphism of polymeric and oligomeric thiophene thin films on silicon oxide substrates from the measured X-ray diffraction patterns.[83] For thin films prepared by dip-coating in a solution of alkylated oligothiophene derivatives in 2-propanol, the diffraction patterns revealed the presence of a polymorph with bent side chains, whereas a mixture of polymorphs with extended and bent side chains was found in films cast from hexane or toluene (Figure 10).[83]

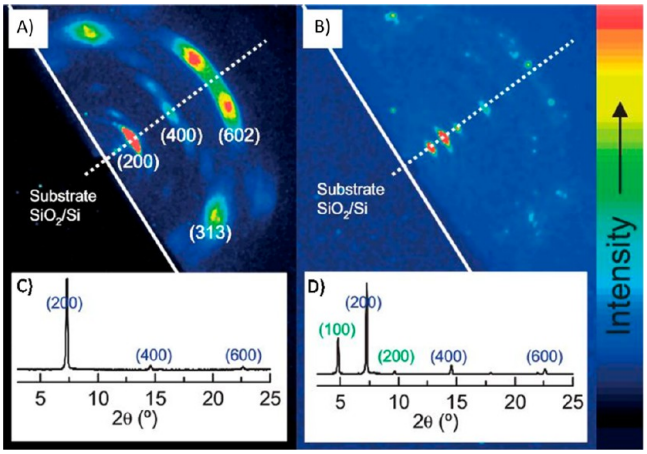

Figure 10. Images of 2D GIXRD measurements (incident X-ray angle = 2.5°) of dip-coated films of **23** (A) from 2-propanol, and (B) from hexane. Insets show thin-film XRD of the corresponding dip-coated films of **23**. (C) from 2-propanol, and (D) from hexane. Reprinted with permission from ref 83. Copyright 2007 Wiley.

In a recently developed resonant soft X-ray scattering method (PSoxS), X-ray scattering is resonantly performed on and off the C1s* transition (the same transition used in NEXAFS to determine aromatic molecule orientations) to obtain the length scale over which the alignment of aromatic cores is largely preserved.[97] Chabinyc and Ade used PSoxs to determine the orientation length scale in PBTTT films and were able to show a direct correlation with FET device performance.[97] In thin films of long oligothiophene derivatives, PSoxS could reveal the length scales over which neighboring grains exhibit small domain angles.[98] Salleo and coworkers demonstrated that this quantity is important to understand the trap-limited charge transport in OFETs of polycrystalline thin films.[98]

6. APPLICATIONS FOR ORGANIC DEVICES

6.1. Organic Field-Effect Transistors. Bao and coworkers systematically investigated the dependency of charge-carrier mobility on the number of terminal α-substituents.[67] They compared the crystal packing and electronic properties of **1**, **2**, and **3** and found that the terminal groups lead to differences in the molecular overlap, which has a dramatic influence on the effective charge transport. The mobility decreases with the increase of substitutions, following the trend, 4T (**1**) > 4TTMS (**2**) > 4T2TMS (**3**) and the predicted charge transport efficiency coincided with the measured one. Figure 11 gives examples of oligothiophene-based materials used in organic transistor and solar cell applications.

Briseno and coworkers recently investigated the effect of backbone length on the transistor performance of oligothiophenes and this was correlated to molecular orientation.[50] The DDQT oligomers (compounds **14**–**19**) showed a significant decrease in crystalline order with increasing oligomer length; charge transport measurements showed a corresponding decrease in mobility with increasing chain length. The mobility trend is comparable with that reported by Neher and coworkers (Figure 12).[99] This indicates that the molecular weight is not a decisive factor for improved carrier mobility in the low molecular weight region, and the increasing in-plane lattice disorder with increasing chain length contributes to the decreased carrier mobilities. The variation of threshold voltage indicates that the quality of the gate dielectric/organic semiconductor interface plays a significant role in terms of device operation. Takimiya and coworkers investigated a series of longer oligothiophenes 20T-40T (compound **26**–**29**), lengths at which the oligomers are considered polymers. These long oligomers formed lamellar packing in the solid state and the measured device mobilities gradually increased with chain extension.[27]

Although the mobilities in thin films formed from the shorter oligomers are limited due to lack of electronic communication between crystallites, oligothiophenes are much more easily crystallized than their polymer counterparts. This allows for the fabrication of transistors with single-crystal conduction channels. For example, single crystals of **15**, the DDQT dimer, were prepared from a hexane solution by the slow addition of ethanol. The long axis of the belt corresponds to the π–π stacking direction, which is the direction of greatest orbital overlap; the backbones of **15** are oriented perpendicular to the long axis of each crystal. The mobilities observed were in the range of 0.01-0.04 $cm^2\ V^{-1}\ s^{-1}$, with an on/off current ratio of 1×10^4. These results are comparable to those reported for thin film transistors based on the analogous polymer, PQT-12, without post- annealing, and are one order of magnitude higher than that of the thin film transistors based on the same material due to the elimination of crystal defects and grain boundaries.[50]

Gentili et al. recently demonstrated the first example of controlled self-assembly of **30**, which contains thioether side groups, by confinement effects.[51,100] This strategy allowed the direct integration of well-ordered supramolecular semiconducting fibers in OFET devices. In the fibers, the oligothiophene backbones lie almost perpendicular to the substrate surface. Although the compound shows low charge mobility, it might provide a technique for the reproducible fabrication of functional devices that requires controlled integration of supramolecular fibers with precise density, orientation, and size for more demanding applications.

Very recently, Guo and cowokers reported a unique asymmetric oligothiophene that is terminated with long alkoxy side chains (compound **31**).[35] The long side chains not only increased the molecular solubility, but also improved the self-assembly properties; the molecule formed lamella-like stacking in the solid state, which allowed optimal intermolecular π–π interactions. The mobility of thin films was ~0.1 $cm^2\ V^{-1}\ s^{-1}$ and increased to 0.2 $cm^2\ V^{-1}\ s^{-1}$ upon annealing, while transistors based on single crystals of the molecule reached 6.0 $cm^2\ V^{-1}\ s^{-1}$.

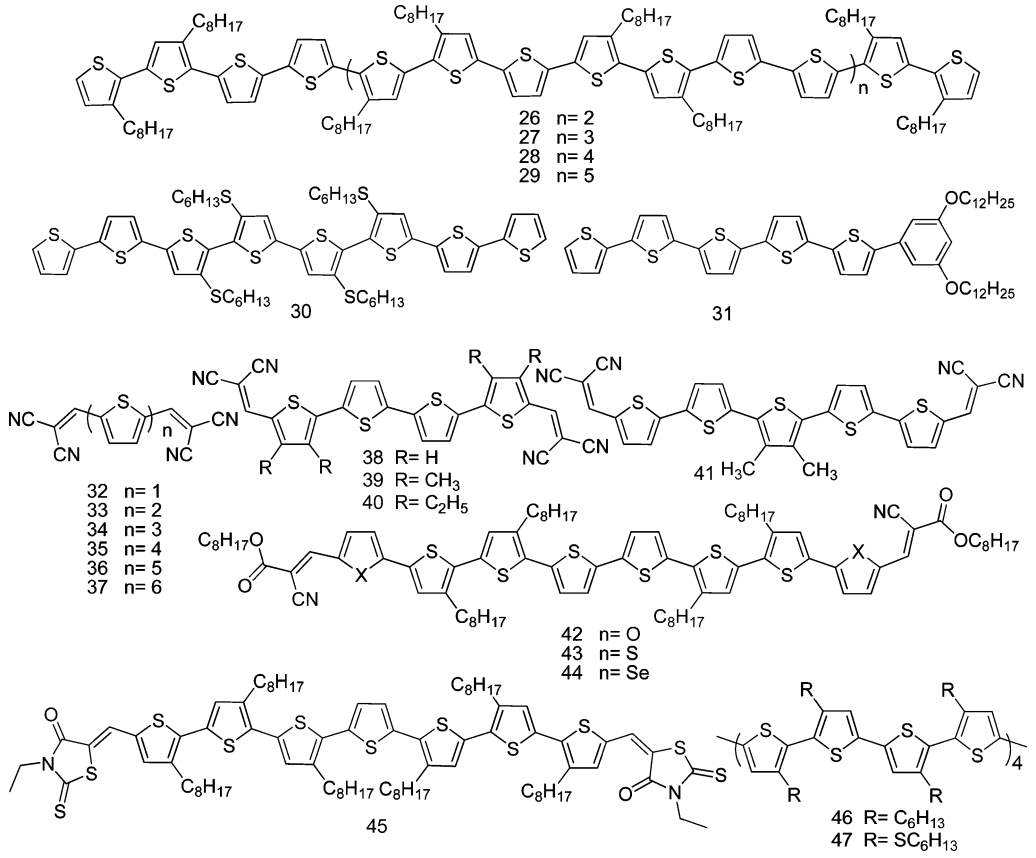

Figure 11. Examples of oligothiophene-based materials for organic transistor and solar cell applications.

Monolayers are an extreme example of thin films that highlight the dependence of charge transport on conduction pathways. The mobility in monolayer transistors is typically orders of magnitude lower than in the corresponding multilayer film due to the structural defects and grain boundaries in the monolayer. Mourran and coworkers investigated monolayer transistors based on **24**, an oligothiophene with branched alkyl chains at the α positions, which is capable of forming crystalline and liquid crystalline phases.[86] They found that the bulkiness of the end groups enhanced the solubility and allowed for the solution deposition and self-assembly of an electrically connected monolayer, resulting in mobilities up to 0.02 $cm^2 V^{-1} s^{-1}$. They also discovered that, in a monolayer, the molecules are tilted at an angle greater than in the bulk crystal. Recently, Mannebach et al. selected **25**, which has linear alkyl substituents at the α positions, as a semiconductor for fabricating monolayer transistors.[85] They discovered that the molecular axis was significantly tilted relative to the surface normal, resulting in a larger in-plane lattice constant. Because the conducting thiophene cores were isolated from the interface by the terminal hexyl chains, the authors attributed the high performance, with mobilities up to 0.032 $cm^2 V^{-1} s^{-1}$, to the reduction in hole scattering. They also found that additional layers did not improve charge transport in the devices; the carrier mobility saturated after the completion of a single monolayer.

6.2. Organic Solar Cells. One popular strategy for tuning the band gap of oligomers is to incorporate electron-withdrawing groups at the α-positions, extending the absorption. Bäuerle and coworkers reported a series of oligomers (**32**-**37**) in which they introduced a strong electron withdrawing unit, DCV, into oligothiophenes and studied their application in organic photovoltaics.[36,59,101] The authors systematically investigated the effect of conjugation length on the solar cell device performance. They observed that, for the longer oligomers (n = 3−6), the V_{OC} gradually decreased with increasing conjugation because of the increasing HOMO level. The shift in energy levels and reduction of the band gap resulted in a clear red-shift and an increase in molar absorptivity as the conjugation length increased.

The effect of crystal packing and intermolecular interactions on the device performance in analogous systems has also been investigated. Hydrogen bonding can also play a role in the crystal packing of substituted oligothiophenes. For example, nitrile residues can act as supramolecular synthons to link molecules into extended ribbons by CN···H interactions.[68] Compounds **38**, **39**, and **40** adopt slipped π-stack arrangement by CN···H interactions, which exert an orientational influence on ribbon packing, preventing a herringbone arrangement (Figure 13). It is should also be noted that the subtle chemical modification leads to great variations in packing arrangements and intermolecular interactions: the number of interactions per molecule in the single crystal is 0.9 for compound **38**, 4 for **39**, and 8 for **40**.[89] These multiple nonbonding short contacts lead to better ordering within crystallites, resulting in a perfect coplanar layer structure. The strong $\pi-\pi$ interaction and electronic coupling increases charge transport; compound **39** showed the best PCE (3.8%). This indicates that the selection of appropriate substituents is necessary to provide efficient molecular packing for high carrier mobility and solar cell efficiency. More recently, these authors reported on a novel series of quinquethiophenes terminated with DCV, in which

dx.doi.org/10.1021/am4060468 | ACS Appl. Mater. Interfaces 2014, 6, 5327−5343

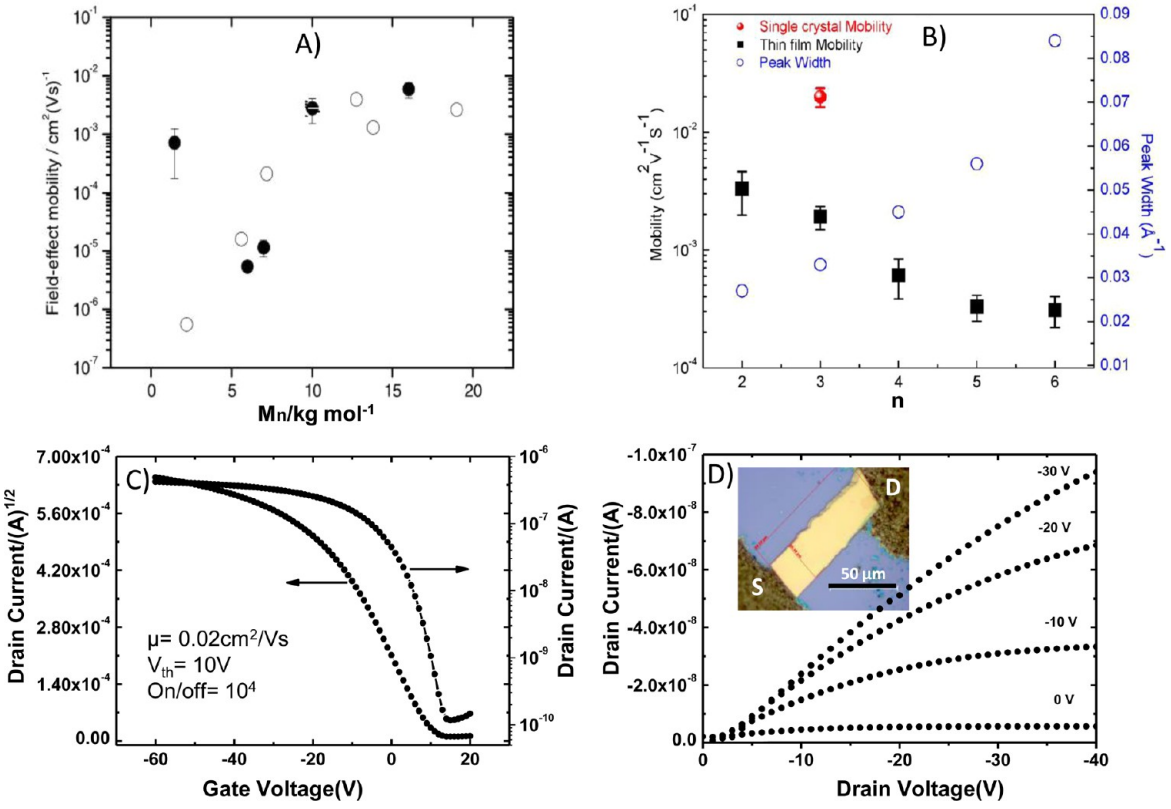

Figure 12. (A) Field-effect mobility in thin films of PQT-12 (solid symbols) and P3HT (open symbols) versus number-average molecular weight. Reprinted with permission from ref 99. Copyright 2009 Springer. (B) Thin-film carrier mobilities of oligothiophenes (black squares) and in-plane peak widths (open circles) as a function of oligomer length. A single-crystal transistor of **16** is shown in red circles. (C) Transfer/square root of current characteristics, and (D) output characteristics of a **16** single-crystal transistor. Inset: single crystal transistor of **16** on Si/SiO_2 (300 nm) with carbon paste as top-contact source-drain electrodes. Reprinted with permission from ref 50. Copyright 2013 American Chemical Society.

Table 2. Summary of the Field-Effect Mobilities (μ), Threshold Voltages (V_T), Current I_{on}/I_{off} Ratios and OFET Device Structure Based on Oligothiophenes

compd	device structure[a]	μ ($cm^2\ V^{-1}\ s^{-1}$)	I_{on}/I_{off}	V_t(V)	ref
1	BG-TC/SCFET	0.23	1×10^7	−6	67
2	BG-TC/SCFET	0.13	1×10^4	−10	67
3	BG-TC/SCFET	0.03	1×10^3	−12	67
15	BG-TC/thin film (solution process)	$(1.0–4.3) \times 10^{-3}$	1×10^3	−0.9 to 0.6	50
16	BG-TC/thin film (solution process)	$(1.7–2.6) \times 10^{-3}$	1×10^3	−0.9 to 0.6	50
15	BG-TC/SCFET	0.01−0.04	1×10^3	−1.3 to 6.7	50
27	BG-TC/thin film (solution process)	8.8×10^{-4}	1×10^3	4.0	27
28	BG-TC/thin film (solution process)	1.3×10^{-3}	1×10^3	5.1	27
29	BG-TC/thin film (solution process)	2.1×10^{-3}	1×10^3	−6.0	27
30	BG-TC/aligned fiber (solution process)	3×10^{-3}	23	−26	100
31	BG-TC/thin film (solution process)	0.2	1×10^5	−11	35
31	BG-TC/SCFET	4	1×10^6	−9	35
24	BG-BC/SAMFET	0.032	1×10^7	4.4	85
25	BG-TC/SAMFET	1×10^{-2}	1×10^4		86

[a]BG-TC, bottom-gate/top-contact; BG-BC, bottom-gate/top-contact; SCFET, single-crystal field effect transistor; SAMFET, self-assembly monolayer field effect transistor.

the positioning of methyl substituents along the conjugated backbone was systematically varied.[34] These oligomers were incorporated into vacuum-processed p−i−n-type BHJ solar cells which exhibited PCEs of 4.8−6.1%. In the solid state, one molecule of **41** interacts with 10 neighboring molecules via 16 well-defined interactions. As expected, the intermolecular interactions again have considerable influence on solar cell efficiency, as they promote better ordering. The PCE of **36** was up to 6.9%, which is one of the highest reported for small molecule OPVs.

To increase the solubility in organic solvents and miscibility with fullerene derivatives, Yang and coworkers reported a series of solution processable small molecules consisting of sexithiophene connected to electron-withdrawing octyl cyanoacetate groups via furan, thiophene, or selenophene linkers (**42**−**44**).[102] All of these small molecules showed high PCEs of

Table 3. Summary of the Short-Circuit Current Density(J_{sc}), Open-Circuit Voltage (V_{oc}), Fill Factor, and Power Efficiency and Solar Cell Device Structures Based on Oligothiophenes

device structure[a]	J_{sc}	V_{oc}	FF	PCE (%)	ref
ITO/C_{60} (15 nm)/**35** (6 nm)/BPAPF (5 nm)/22:NDP9 (10 wt %, 50 nm)/NDP9 (1 nm)/Au	2.9	0.97	0.42	1.2	59
ITO/C_{60} (15 nm)/**36** (6 nm)/ BPAPF (5 nm)/22:NDP9 (10 wt %, 50 nm)/NDP9 (1 nm)/Au	5.1	0.97	0.52	2.6	59
ITO/C_{60} (15 nm)/**37** (6 nm)/ BPAPF (5 nm)/22:NDP9 (10 wt %, 50 nm)/NDP9 (1 nm)/Au	4.8	0.91	0.64	2.8	59
ITO/C_{60} (15 nm)/**38**:C_{60}(20 nm)/BPAPF (5 nm)/BPAPF:NDP9 (10 wt %, 50 nm)/NDP9 (1 nm)/Au	0.92	3.5	0.47	1.5	89
ITO/C_{60} (15 nm)/**39**:C_{60}(20 nm)/BPAPF (5 nm)/BPAPF:NDP9 (10 wt %, 50 nm)/NDP9 (1 nm)/Au	0.98	6.5	0.59	3.8	89
ITO/C_{60} (15 nm)/**40**:C_{60}(20 nm)/BPAPF (5 nm)/BPAPF:NDP9 (10 wt %, 50 nm)/NDP9 (1 nm)/Au	0.98	5.7	0.39	2.2	89
ITO/C_{60} (15 nm)/**41**:C_{60}(20 nm)/BPAPF (5 nm)/BPAPF:NDP9 (10 wt %, 50 nm)/NDP9 (1 nm)/Au	0.95	11.5	0.63	6.9	34
ITO/PEDOT:PSS (40 nm)/**42**:$PC_{71}BM$ (110 nm)/LiF/Al	6.34	0.78	0.64	3.18	102
ITO/PEDOT:PSS (40 nm)/**43**:$PC_{71}BM$ (120 nm)/LiF/Al	7.43	0.85	0.72	4.52	102
ITO/PEDOT:PSS (40 nm)/**44**:$PC_{71}BM$ (120 nm)/LiF/Al	10.79	0.85	0.67	6.15	102
ITO/PEDOT:PSS (40 nm)/**45**:PCBM (65-120 nm)/LiF/Al	13.98	0.92	0.47	6.1	103
ITO/PEDOT:PSS (40 nm)/**46**:PCBM (100 nm) /Al	5.13	0.64	0.46	1.49	105
ITO/PEDOT:PSS (40 nm)/**47**:PCBM (100 nm) /Al	0.06	0.56	0.25	0.01	105

[a]BPAPF = 9,9-bis[4-(N,N-bis-biphenyl-4-yl-amino)phenyl]-9H-fluorene; NDP9 is a p-type donor compound sold by Novaled, AG.[36]

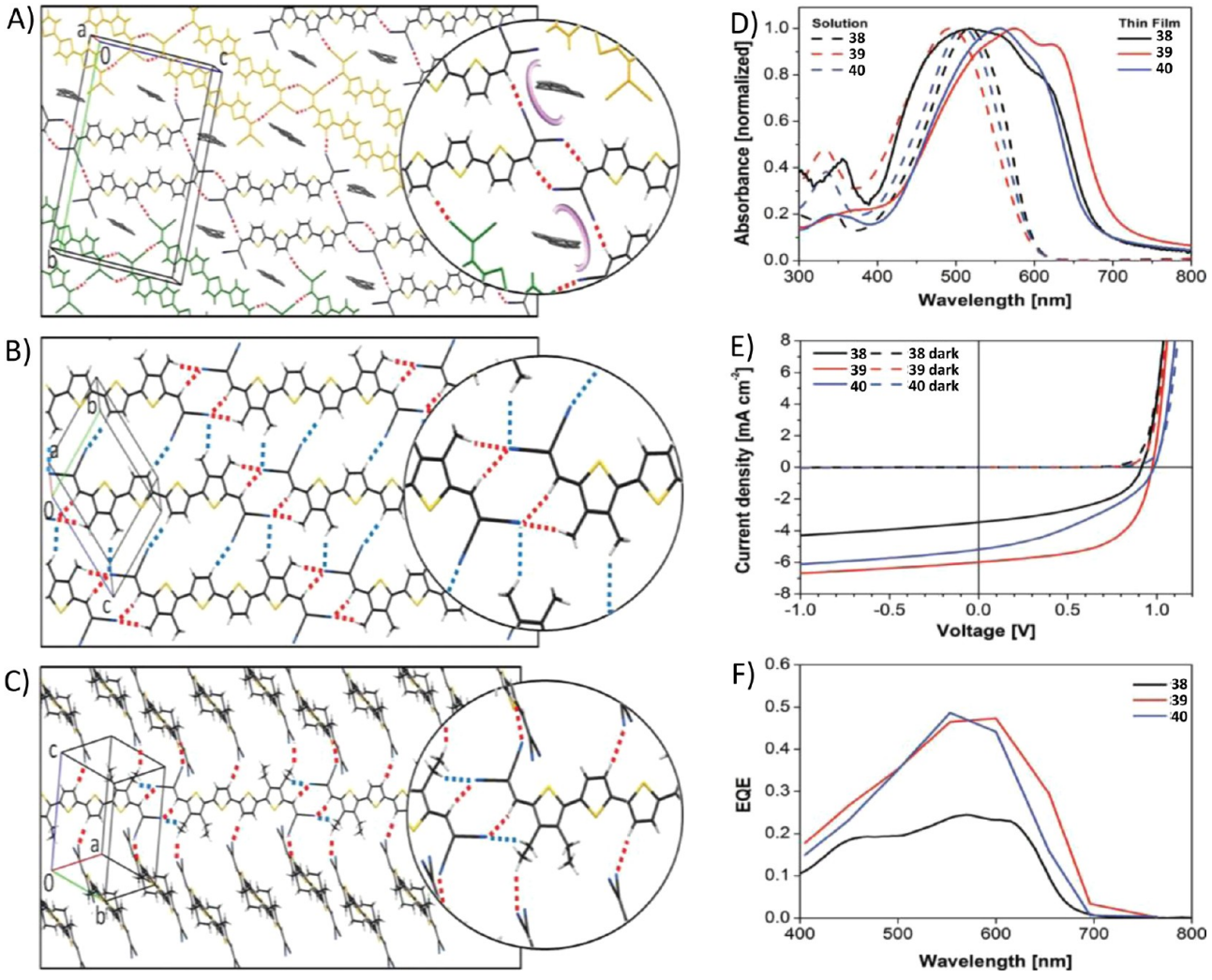

Figure 13. X-ray structure analysis of quaterthiophenes (A) **38**, (B) **39**, and (C) **40** in the molecular plane of the single crystals and details of the short atomic distances (insets). (C) Absorption spectra of quaterthiophenes **38**–**40** measured in tetrachloroethane at 80 °C (dashed lines) and in 30 nm thin films (solid lines). (D) *J*–*V* characteristics of bulk heterojunction solar cells containing oligomers **38**–**40** as donor materials. (E) EQE spectra of BHJ solar cells comprising **38**–**40**. Reprinted with permission from ref 89. Copyright 2012 Wiley.

3.18–6.15% in OPVs with $PC_{71}BM$ as the acceptor. Compared to **42** and **43**, compound **44** provided stronger heteroaromatic interactions which lead to a considerable red shift of the maximum absorption. The best conditions were a D:A blend ratio of 1:1.15 with PDMS as an additive to tune the morphology, which produced a device with V_{oc} = 0.85 V, J_{sc}

dx.doi.org/10.1021/am4060468 | ACS Appl. Mater. Interfaces 2014, 6, 5327–5343

= 10.79 mA/cm^2, and FF = 67.1%, and PCE = 6.15%. Chen and coworkers reported a series of solution processable septithiophenes end-capped with dye building blocks to obtain high solar absorption.[37,103,104] These compounds exhibited higher absorption, which lead to high J_{sc}. Compound **44** achieved PCEs of about 6.1% with PCBM. Beyond the enhanced absorption, the performance was ascribed to the better network morphology and balanced charge transport in the active layers.

Barbarella and coworkers investigated two regioregular thiophene hexadecamers bearing head-to-head and alkyl chains, **46**, and thioalkyl chains, **47**, as donor molecules for solution processed solar cells.[105] The sulfur atoms acted as a "reservoir" of electrons to compensate for the decrease in electron delocalization caused by the backbone torsion. Compared to **46**, the absorption of **47** is remarkably red-shifted and the redox potentials decrease by 0.38 V. The authors note that the λ_{max} value and redox potentials are similar to those of head-to-tail poly(3-hexylthiophene). The device based on **47** and PCBM exhibited V_{oc} = 0.64 V, J_{sc} = 5.13 mA/cm^2, FF = 64%, and PCE = 1.49%.

7. CONCLUSIONS AND FUTURE RESEARCH PERSPECTIVE

In parallel to the remarkable developments surrounding polythiophenes as organic semiconductor materials, oligothiophenes have also been investigated as promising active semiconductor materials for OFETs and OPVs. Structurally defined, monodisperse oligothiophenes are excellent model compounds for establishing valuable structure-property relationships which can be extrapolated to their polymer analogs. Although the synthesis of oligothiophenes involves multiple steps, these defect-free materials are easy to modify with different moieties, providing novel functionality beyond the thiophene core. This leads some to believe that functionalized oligothiophenes should be considered as the next generation of advanced conjugated materials for organic electronic devices, especially as the performance of solar cells based on these small molecules is comparable to that of benchmark polymers.

Although the synthesis of oligothiophenes is currently tedious and time consuming, especially for longer, more absorptive oliothiophenes (more than 8 units)-new synthetic methods, including high-efficiency catalyst systems, should continue to be explored. Much work also still remains to be done in modifying the structure of these materials to tune their absorption, solubility, morphology and crystallinity. A deeper understanding of the relationship between the molecular structure and crystal packing should be developed in order to design new materials for high-performance devices. For example, the understanding of the electronic structure and charge-transport properties of single crystals remains incomplete for even simple systems, such as ß-alkylated oligothiophenes. This is in part because the growth of crystals of the longer oligothiophenes for x-ray diffraction remains challenging. Beyond that, it is known that molecules with flexible moieties, such as alkyl chains, show a particularly strong tendency toward polymorphism which can considerably impact the device performance. Therefore, it is critical to understand and control polymorphism in thin films. Fortunately, there are many talented synthetic chemists and characterization experts working to further our understanding of these promising molecules.

Density functional theory (DFT) calculations are routinely applied to elucidate the electronic properties of conjugated polythiophenes using the "oligomer thiophene approach".[106] Although, DFT calculations can also provide information on electronic structure (bandgap, doping energy, structure, orbital energies/ionization potentials, reorganization energy, electronic spectra, and so on), the calculated values are method, which is strongly dependent on the computational level used.[107] There are important deficiencies with common DFT approaches related to the delocalization errors and the spurious lowering of charge transfer state energies that can hinder the quantitative predictability of common DFT functionals for conjugated oligomers/polymers. An example of this can be the torsion potentials in the electronic ground state.[108] DFT are not useful in predicting molecular packing, 2D/3D structure and/or properties which are related to the bulk. The determination of crystal structures with computational tools is still in its infancy and many of the methods currently employed have serious limitations with regard to the pi-pi interactions important for packing and morphology in conjugated oligomers/polymers. Oligomer studies are critical to understanding the properties of the conjugated polymers (especially electronic properties), but further advances in theoretical methods are needed to: (i) improve electronic structure methods to introduce quantitative/predictive accuracy to computed electronic properties, and (ii) improve (probably molecular mechanics) methods for describing the $\pi-\pi$ interactions and for predicting packing morphologies.

AUTHOR INFORMATION

Corresponding Author

*E-mail: abriseno@mail.pse.umass.edu.

Notes

The authors declare no competing financial interest.

ACKNOWLEDGMENTS

We dedicate this work in memory of our friend and colleague, Professor Michael Bendikov (1971–2013). A.L.B thanks the National Science Foundation for primary support of this work (DMR-1112455), and Center for Hierarchical Manufacturing, which provided support for N.S.C. (CMMI-0531171). We thank Dr. John Sears from Georgia Tech for discussion on the future of computational studies.

REFERENCES

(1) Beaujuge, P. M.; Fréchet, J. M. J. Molecular Design and Ordering Effects in π-Functional Materials for Transistor and Solar Cell Applications. *J. Am. Chem. Soc.* **2011**, *133*, 20009–20029.

(2) Heeney, M.; Bailey, C.; Genevicius, K.; Shkunov, M.; Soarrow, D.; Tierney, S.; McCulloch, I. Stable Polythiophene Semiconductor Incorporating Thieno[2,3-*b*]thiophene. *J. Am. Chem. Soc* **2005**, *127*, 1078–1079.

(3) McCullough, R. D. The Chemistry of Conducting Polythiophenes. *Adv. Mater* **1998**, *10*, 93–116.

(4) *Electronic Materials: The Oligomer Approach*; Müllen, K.; Wenger, G., Eds.; Wiley-VCH: Weinheim, Germany, 1997.

(5) Kline, R. J.; McGehee, M. D.; Kadnikova, E. N.; Liu, J. S.; Fréchet, J. M. J. Controlling the Field-Effect Mobility of of Regioregular Polythiophene by Changing the Molecular Weight. *Adv. Mater.* **2003**, *15*, 1519–1522.

(6) Prosa, T. J.; Winokur, M. J.; Moulton, J.; Smith, P.; Heeger, A. J. X-Ray Structural Studies of Poly(3-alkylthiophenes): An Example of an Inverse Comb. *Macromolecules* **1992**, *25*, 4364–4372.

(7) Meille, S. V.; Romita, V.; Caronna, T.; Lovinger, A. J.; Catellani, M.; Belobrzeckaja, L. Influence of Molecular Weight and Regioregularity on the Polymorphic Behavior of Poly(3- decylthiophenes). *Macromolecules* **1997**, *30*, 7898−7905.
(8) Kline, R. J.; McGehee, M. D.; Kadnikova, E. N.; Liu, J. S.; Fréchet, J. M. J.; Toney, M. F. Dependence of Regioregular Poly(3-hexylthiophene) Film Morphology and Field-Effect Mobility on Molecular Weight. *Macromolecules* **2005**, *38*, 3312−3319.
(9) Kline, R. J.; Delongchamp, D. M.; Fischer, D. A.; Lin, E. K.; Richter, L. J.; Chabinyc, M. L.; Toney, M. F.; Heeney, M.; McCulloch, I. Critical Role of Side-Chain Attachment Density on the Order and Device Performance of Polythiophenes. *Macromolecules* **2007**, *40*, 7960−7965.
(10) Zen, A.; Pflaum, J.; Hirschmann, S.; Zhuang, W.; Jaiser, F.; Asawapirom, U.; Rabe, J. P.; Scherf, U.; Neher, D. Effect of Molecular Weight and Annealing of Poly(3-hexylthiophene)s on the Performance of Organic Field-Effect Transistors. *Adv. Funct. Mater.* **2004**, *14*, 757−764.
(11) Joshi, S.; Grigorian, S.; Pietsch, U.; Pingel, P.; Zen, A.; Neher, D.; Scherf, U. Thickness Dependence of the Crystalline Structure and Hole Mobility in Thin Films of Low Molecular Weight Poly(3-hexylthiophene). *Macromolecules* **2008**, *41*, 6800−6808.
(12) Lim, J. A.; Liu, F.; Ferdous, S.; Muthukumar, M.; Briseno, A. L. Polymer Semiconductor Crystals. *Mater. Today* **2010**, *13*, 14−24.
(13) Coffin, R. C.; Peet, J.; Rogers, J.; Bazan, G. C. Streamlined Microwave-Assisted Preparation of Narrow-Bandgap Conjugated Polymers for High-Performance Bulk Heterojunction Solar Cells. *Nat. Chem.* **2009**, *1*, 657−661.
(14) Schilinsky, P.; Asawapirom, U.; Scherf, U.; Biele, M.; Brabec, C. J. Influence of the Molecular Weight of Poly(3-hexylthiophene) on the Performance of Bulk Heterojunction Solar Cells. *Chem. Mater.* **2005**, *17*, 2175−2180.
(15) Thompson, B. C.; Fréchet, J. M. J. Polymer−Fullerene Composite Solar Cells. *Angew. Chem., Int. Ed* **2008**, *47*, 58−77.
(16) Li, G.; Shrotriya, V.; Huang, J. S.; Yao, Y.; Moriarty, K.; Yang, Y. High-Efficiency Solution Processable Polymer Photovoltaic Cells by Self-Organization of Polymer Blends. *Nat. Mater.* **2005**, *4*, 864−868.
(17) He, Z.; Zhong, C.; Su, S.; Xu, M.; Wu, H.; Cao, Y. Enhanced Power-Conversion Efficiency in Polymer Solar Cells Using an Inverted Device Structure. *Nat. Photonics* **2012**, *6*, 591−595.
(18) Dou, L.; You, J.; Yang, J.; Chen, C.; He, Y.; Murase, S.; Moriarty, T.; Emery, K.; Li, G.; Yang, Y. Tandem Polymer Solar Cells Featuring a Spectrally Matched Low-Bandgap Polymer. *Nat. Photonics* **2012**, *6*, 180−185.
(19) Chen, H.; Guo, Y.; Yu, G.; Zhao, Y.; Zhang, J.; Gao, D.; Liu, H.; Liu, Y. Highly π-Extended Copolymers with Diketopyrrolopyrrole Moieties for High-Performance Field-Effect Transistors. *Adv. Mater.* **2012**, *24*, 4618−4622.
(20) Lei, T.; Cao, Y.; Zhou, X.; Peng, Y.; Bian, J.; Pei, J. Systematic Investigation of Isoindigo-Based Polymeric Field-Effect Transistors: Design Strategy and Impact of Polymer Symmetry and Backbone Curvature. *Chem. Mater.* **2012**, *24*, 1762−1770.
(21) Lei, T.; Cao, Y.; Fan, Y.; Liu, C.; Yuan, S.; Pei, J. High-Performance Air-Stable Organic Field-Effect Transistors: Isoindigo-Based Conjugated Polymers. *J. Am. Chem. Soc.* **2011**, *133*, 6099−6101.
(22) Mei, J.; Kim, D. H.; Ayzner, A. L.; Toney, M. F.; Bao, Z. Siloxane-Terminated Solubilizing Side Chains: Bringing Conjugated Polymer Backbones Closer and Boosting Hole Mobilities in Thin-Film Transistors. *J. Am. Chem. Soc.* **2011**, *133*, 20130−30133.
(23) Wang, S.; Kiersnowski, A.; Pisula, W.; Müllen, K. Microstructure Evolution and Device Performance in Solution-Processed Polymeric Field-Effect Transistors: The Key Role of the First Monolayer. *J. Am. Chem. Soc.* **2012**, *134*, 4015−4018.
(24) Mishra, A.; Ma, C.-Q.; Bäuerle, P. Functional Oligothiophenes: Molecular Design for Multidimensional Nanoarchitectures and Their Applications. *Chem. Rev.* **2009**, *109*, 1141−1276.
(25) Mena-Osteritz, E.; Meyer, A.; Langeveld-Voss, B. M. W.; Janssen, R. A. J.; Meijer, E. W.; Bäuerle, P. Two-Dimensional Crystals of Poly(3-Alkyl- thiophene)s: Direct Visualization of Polymer Folds in Submolecular Resolution. *Angew. Chem., Int. Ed.* **2000**, *39*, 2679−2684.
(26) Bäuerle, P.; Fischer, T.; Bildlingmeier, B.; Stabel, A.; Rabe, J. Oligothiophenes—Yet Longer? Synthesis, Characterization, and Scanning Tunneling Microscopy Images of Homologous, Isomerically Pure Oligo(alkylthiophene)s. *Angew. Chem. Int. Ed.* **1995**, *34*, 303−307.
(27) Takimiya, K.; Sakamoto, K.; Otsubo, T.; Kunugi, Y. Thin Film Characteristics and FET Performances of β-Octyl-substituted Long Oligothiophenes. *Chem. Lett.* **2006**, *35*, 942−943.
(28) Izumi, T.; Kobashi, S.; Takimiya, K.; Aso, Y.; Otsubo, T. Synthesis and Spectroscopic Properties of a Series of β-Blocked Long Oligothiophenes up to the 96-mer: Revaluation of Effective Conjugation Length. *J. Am. Chem. Soc.* **2003**, *125*, 5286−5287.
(29) Wang, Q. L.; Qu, Y.; Tian, H. K.; Geng, Y. H.; Wang, F. S. Iterative Binomial Synthesis of Monodisperse Polyfluorenes up to 64-mers and Their Chain-Length- Dependent Properties. *Macromolecules* **2011**, *44*, 1256−1260.
(30) Azumi, R.; Götz, G.; Debaerdemaeker, T.; Bäuerle, P. Coincidence of the Molecular Organization of β-Substituted Oligothiophenes in Two-Dimensional Layers and Three-Dimensional Crystals. *Chem.—Eur. J.* **2000**, *6*, 735−744.
(31) Azumi, R.; Mena-Osteritz, E.; Boese, R.; Benet-Buchholz, J.; Bäuerle, P. The Longest Oligothiophene Ever Examined by X-Ray Structure Analysis. *J. Mater. Chem* **2006**, *16*, 728−735.
(32) Horowitz, G.; Bachet, B.; Yassar, A.; Lang, P.; Dmanze, F.; Fave, J. L.; Gamier, F. Growth and Characterization of Sexithiophene Single Crystals. *Chem. Mater* **1995**, *7*, 1337−1341.
(33) *Handbook of Thiophene-Based Materials: Applications in Organic Electronics and Photonics*; Perepichka, I. F.; Perepichka, D. F., Eds.; Wiley: Chichester, U.K., 2009.
(34) Fitzner, R.; Mena-Osteritz, E.; Mishra, A.; Schulz, G.; Reinold, E.; Weil, M.; Körner, C.; Ziehlke, H.; Elschner, C.; Leo, K.; Riede, M.; Pfeiffer, M.; Uhrich, C.; Bäuerle, P. Correlation of π-Conjugated Oligomer Structure with Film Morphology and Organic Solar Cell Performance. *J. Am. Chem. Soc.* **2012**, *134*, 11064−11067.
(35) Dong, S.; Zhang, H.; Yang, L.; Bai, M.; Yao, Y.; Chen, H.; Gan, L.; Yang, T.; Jiang, H.; Hou, S.; Wan, L.; Guo, X. Solution-Crystallized Organic Semiconductors with High Carrier Mobility and Air Stability. *Adv. Mater.* **2012**, *24*, 5576−5580.
(36) Mishra, A.; Bäuerle, P. Small Molecule Organic Semiconductors on the Move: Promises for Future Solar Energy Technology. *Angew. Chem., Int. Ed.* **2012**, *51*, 2020−2067.
(37) Chen, Y.; Wan, X.; Long, G. High Performance Photovoltaic Applications Using Solution-Processed Small Molecules. *Acc. Chem. Res.* **2013**, *46*, 2645−2655.
(38) Usta, H.; Facchetti, A.; Marks, T. J. *n*-Channel Semiconductor Materials Design for Organic Complementary Circuits. *Acc. Chem. Re.s* **2011**, *44*, 501−510.
(39) Osaka, I.; McCullough, R. Advances in Molecular Design and Synthesis of Regioregular Polythiophenes. *Acc. Chem. Res.* **2008**, *41*, 1202−1214.
(40) Katz, H.; Bao, Z.; Gilat, S. L. Synthetic Chemistry for Ultrapure, Processable, and High-Mobility Organic Transistor Semiconductors. *Acc. Chem. Res* **2001**, *34*, 359−369.
(41) Allard, S.; Forster, M.; Souharce, B.; Thiem, H.; Scherf, U. Organic Semiconductors for Solution-Processable Field-Effect Transistors (OFETs). *Angew. Chem., Int. Ed* **2008**, *47*, 4070−4098.
(42) Barbarella, G.; Zambianchi, M.; Di Toro, R.; Colonna, M.; Iarossi, D.; Goldoni, F.; Bongini, A. Regioselective Oligomerization of 3-(Alkylsulfanyl)thiophenes with Ferric Chloride. *J. Org. Chem* **1996**, *61*, 8285−8292.
(43) Wei, Y.; Chan, C.; Tian, J.; Jang, G.; Hsueh, K. Electrochemical Polymerization of Thiophenes in the Presence of Bithiophene or Terthiophene: Kinetics and Mechanism of the Polymerization. *Chem. Mater.* **1991**, *3*, 888−897.
(44) Roncali, J. Synthetic Principles for Bandgap Control in Linear π-Conjugated Systems. *Chem. Rev.* **1997**, *97*, 173−206.

(45) Engelmann, G.; Jugelt, W.; Kossmehl, G.; Welzel, H.; Tschuncky, P.; Heinze, J. Doped Polymers by Oxidative Polymerization. 4. Oxidative Coupling of Methylated Oligothiophenes by $FeCl_3 \cdot 6H_2O$ as a Model Reaction for the Oxidative Polymerization of Thiophene Derivatives. *Macromolecules* **1996**, *29*, 3370−3375.
(46) Zhang, F.; Bäuerle, P. A Controlled Approach to Well-Defined Oligothiophenes via Oxidatively Induced Reductive Elimination of Stable Pt(II) Oligothienyl Complexes. *J. Am. Chem. Soc* **2007**, *129*, 3090−3091.
(47) Takahashi, M.; Masui, K.; Sekiguchi, H.; Kobayashi, N.; Mori, A.; Funahashi, M.; Tamaoki, N. Palladium-Catalyzed C−H Homocoupling of Bromothiophene Derivatives and Synthetic Application to Well-Defined Oligothiophenes. *J. Am. Chem. Soc* **2006**, *128*, 10930−10933.
(48) Masuda, N.; Tanba, S.; Sugie, A.; Monguchi, D.; Koumura, N.; Hara, K.; Mori, A. Stepwise Construction of Head-to-Tail-Type Oligothiophenes via Iterative Palladium-Catalyzed CH Arylation and Halogen Exchange. *Org. Lett* **2009**, *11*, 2297−2300.
(49) Tanaka, S.; Tamba, S.; Tanaka, D.; Sugie, A.; Mori, A. Synthesis of Well-Defined Head-to-Tail-Type Oligothiophenes by Regioselective Deprotonation of 3-Substituted Thiophenes and Nickel-Catalyzed Cross-Coupling Reaction. *J. Am. Chem. Soc* **2011**, *133*, 16734−16737.
(50) Zhang, L.; Colella, N.; Liu, F.; Trahan, S.; Baral, J.; Winter, H.; Mannsfeld, S.; Briseno, A. Synthesis, Electronic Structure, Molecular Packing/Morphology Evolution, and Carrier Mobilities of Pure Oligo-/Poly(alkylthiophenes). *J. Am. Chem. Soc* **2013**, *135*, 844−854.
(51) Di Maria, F.; Olivelli, P.; Gazzano, M.; Zanelli, A.; Biasiucci, G.; Gigli, G.; Gentili, D.; D'Angelo, P.; Cavallini, M.; Barbarella, G. A Successful Chemical Strategy To Induce Oligothiophene Self-Assembly into Fibers with Tunable Shape and Function. *J. Am. Chem. Soc* **2011**, *133*, 8654−8661.
(52) Koch, F.P.V.; Smith, P.; Heeney, M. Fibonacci's Route to Regioregular Oligo(3-hexylthiophene)s. *J. Am. Chem. Soc.* **2013**, *135*, 13695−13698.
(53) Rieke, R.; Kim, S.; W, X. Direct Preparation of 3-Thienyl Organometallic Reagents: 3-Thienylzinc and 3-Thienylmagnesium Iodides and 3-Thienylmanganese Bromides and Their Coupling Reactions. *J. Org. Chem.* **1997**, *62*, 6921−6927.
(54) Wenz, G.; Mueller, M. A.; Schmidt, M.; Wegner, G. Structure of Poly (diacetylenes) in Solution. *Macromolecules* **1984**, *17*, 837−850.
(55) Meier, H.; Stalmach, U.; Kolshorn, H. Effective conjugation length and UV/vis spectra of oligomers. *Acta Polym.* **1997**, *48*, 379−384.
(56) Zade, S. S.; Bendikov, M. From Oligomers to Polymer: Convergence in the HOMO−LUMO Gaps of Conjugated Oligomers. *Org. Lett.* **2006**, *8*, 5243−5246.
(57) Oliveira, E. F. d.; Lavarda, F. C. Structure of P3HT in the Solid State. *J. Polym. Sci., Part B: Polym. Phys.* **2013**, *51*, 1350−1354.
(58) Bidan, G.; De Nicola, A.; Enée, V.; Guillerez, S. Synthesis and UV−Visible Properties of Soluble Regioregular Oligo(3-octylthiophenes), Monomer to Hexamer. *Chem. Mater.* **1998**, *10*, 1052−1058.
(59) Fitzner, R.; Reinold, E.; Mishra, A.; Mena-Osteritz, E.; Ziehlke, H.; Körner, C.; Leo, K.; Riede, M.; Weil, M.; Tsaryova, O.; Weiß, A.; Uhrich, C.; Pfeiffer, M.; Bäuerle, P. Dicyanovinyl−Substituted Oligothiophenes: Structure-Property Relationships and Application in Vacuum- Processed Small Molecule Organic Solar Cells. *Adv. Funct. Mater.* **2011**, *21*, 897−910.
(60) Schulze, K.; Uhrich, C.; Schüppel, R.; Leo, K.; Pfeiffer, M.; Brier, E.; Reinold, E.; Bäuerle, P. Efficient Vacuum-Deposited Organic Solar Cells Based on a New Low-Bandgap Oligothiophene and Fullerene C_{60}. *Adv. Mater.* **2006**, *18*, 2872−2875.
(61) Fichou, D. Structural Order in Conjugated Oligothiophenes and its Implications on Opto-electronic Devices. *J. Mater. Chem.* **2000**, *10*, 571−588.
(62) Tan, L.; Zhang, L.; Jiang, X.; Yang, X.; Wang, L.; Wang, Z.; Li, L.; Hu, W.; Shuai, Z.; Li, L.; Zhu, D. A Densely and Uniformly Packed Organic Semiconductor Based on Annelated β-Trithiophenes for High- Performance Thin Film Transistors. *Adv. Funct. Mater.* **2009**, *19*, 272−276.
(63) Zhang, L.; Tan, L.; Wang, Z.; Hu, W.; Zhu, D. High-Performance, Stable Organic Field-Effect Transistors Based on *trans*-1,2-(Dithieno[2,3-*b*:3′,2′- *d*]thiophene)ethene. *Chem. Mater* **2009**, *21*, 1993−1999.
(64) Coropceanu, V.; Cornil, J.; Da Silva Filho, D. A.; Olivier, Y.; Silbey, R.; Brédas, J. L. Charge Transport in Organic Semiconductors. *Chem. Rev.* **2007**, *107*, 926−952.
(65) Wang, C.; Dong, H.; Hu, W.; Liu, Y.; Zhu, D. Semiconducting π-Conjugated Systems in Field-Effect Transistors: A Material Odyssey of Organic Electronics. *Chem. Rev* **2012**, *112*, 2208−2267.
(66) Akkerman, H. B.; Mannsfeld, S. C. B.; Kaushik, A. P.; Verploegen, E.; Burnier, L.; Zoombelt, A. P.; Saathoff, J. D.; Hong, S.; Atahan-Evrenk, S.; Liu, X.; Aspurn-Guzik, A.; Toney, M. F.; Clancy, P.; Bao, Z. Effects of Odd−Even Side Chain Length of Alkyl-Substituted Diphenylbithiophenes on First Monolayer Thin Film Packing Structure. *J. Am. Chem. Soc.* **2013**, *135*, 11006−11014.
(67) Reese, C.; Roberts, M.; Parkin, S. P.; Bao, Z. Tuning Crystalline Solid-State Order and Charge Transport via Building-Block Modification of Oligothiophenes. *Adv. Mater.* **2009**, *21*, 3678−3681.
(68) Barclay, T. M.; Cordes, A. W.; Mackinnon, C. D.; Oakley, R. T.; Reed, R. W. Oligothiophenes End-Capped by Nitriles. Preparation and Crystal Structures of α,ω- Dicyanooligothiophenes $NC(C_4H_2S)_nCN$ (n = 3−6). *Chem. Mater* **1997**, *9*, 981−990.
(69) Barbarella, G.; Zamhianchi, M.; Di Toro, R.; Colonna, M.; Antolini, L.; Bongini, A. Functionalization of Sexithiophene with Electron-donating Methylsulphanyl Groups. *Adv. Mater.* **1996**, *8*, 327−331.
(70) Liao, J.; Benz, M.; LeGoff, E.; Kunutzidis, M. G. Oligothiophenes as Models for Polythiophenes. The Crystal and Molecular Structures of 3″, 4″- Dibutylpentathiophene and 3′, 3″, 4′, 4″-Tetrabutylhexathiophene. *Adv. Mater.* **1994**, *6*, 135−138.
(71) Facchetti, A.; Yoon, M.; Stern, C. L.; Hutchison, G. R.; Ratner, M.; Marks, T. J. Building Blocks for N-Type Molecular and Polymeric Electronics. Perfluoroalkyl- versus Alkyl- Functionalized Oligothiophenes (nTs; n = 2−6). Systematic Synthesis, Spectroscopy, Electrochemistry, and Solid-State Organization. *J. Am. Chem. Soc.* **2004**, *126*, 13480−13501.
(72) Barbarella, G.; Zambianchi, M.; Bongini, A.; Antonili, L. Crystal Structure of 4,4′,3″,4‴-Tetramethyl2,2′:5′,2″:5″,2‴-tetrathiophene: A Comparison with the Conformation in Solution. *Adv. Mater.* **1992**, *4*, 282−285.
(73) Barbarella, G.; Bongini, A.; Zambianchi, M. Conformation and Optical Absorption Properties of Thiophene Oligomers: ^{13}C-NMR, UV, and MMP2 Calculations of Di- and Tetramethyl-quaterthiophenes. *Adv. Mater.* **1991**, *3*, 494−496.
(74) Destri, S.; Ferro, D. R.; Khotinal, I. A.; Porzio, W.; Farina, A. Tetrahexylsexithiophene: Crystal Structure and Molecular Mechanics Calculations. *Macromol. Chem. Phys.* **1998**, *199*, 1973−1979.
(75) Herrema, J. K.; Wilderman, J.; Van Bolhuis, F.; Hadziioannou, G. Synthesis and Crystal Structures of Two Dialkyl-substituted Sexithiophenes. *Synth. Met.* **1993**, *60*, 239−248.
(76) Kurata, T.; Mohri, T.; Takimiya, K.; Otsubo, T. Conductive, Magnetic, and Optical Properties of Sterically Hindered Dodecithiophenes. Evidence for the Coexistence of Bipolaron and π-Dimer. *Bull. Chem. Soc. Jpn.* **2007**, *80*, 1799−1807.
(77) Dunitz, J.; Bernstein, J. Disappearing Polymorphs. *Acc. Chem. Res.* **1995**, *28*, 193−200.
(78) Mas-Torrent, M.; Rovira, C. Role of Molecular Order and Solid-State Structure in Organic Field-Effect Transistors. *Chem. Rev.* **2011**, *111*, 4833−4856.
(79) Desiraju, G. R. Supramolecular Synthons in Crystal Engineering—A New Organic Synthesis. *Angew. Chem., Int. Ed.* **1995**, *34*, 2311−2327.
(80) Antolini, L.; Horowitz, G.; Kouki, F.; Garnier, F. Polymorphism in Oligothiophenes with an Even Number of Thiophene Subunits. *Adv. Mater.* **1998**, *10*, 382−385.
(81) Barbarella, G.; Zambianchi, M.; del Fresno, M.; Marimon, I.; Antolini, L.; Bongini, A. Conformational Polymorphism of Oligothiophenes: X-ray Structure of the Monoclinic Form of 3, 3′, 4″, 3‴-

Tetrakis(methylsulfany-l)2, 2′:5″, 2″:5″, 2‴-Quaterthiophene. *Adv. Mater.* **1997**, *9*, 484−487.
(82) Barbarella, G.; Zambianchi, M.; Antolini, L.; Ostoja, P.; Maccagnai, P.; Bongini, A.; Marseglia, E. A.; Tedesco, E.; Gigli, G.; Cingolani, R. Solid-State Conformation, Molecular Packing, and Electrical and Optical Properties of Processable *β*- Methylated Sexithiophenes. *J. Am. Chem. Soc* **1999**, *121*, 8920−8926.
(83) Pan, H.; Liu, P.; Li, Y.; Wu, Y.; Ong, B. S.; Xu, G. Unique Polymorphism of Oligothiophenes. *Adv. Mater* **2007**, *19*, 3240−3243.
(84) Elschner, C.; Schrader, M.; Fitzner, R.; Levin, A.; Bäuerle, P.; Andrienko, D.; Leo, K.; Riede, M. Molecular Ordering and Charge Transport in a Dicyanovinyl-substituted Quaterthiophene Thin Film. *RSC Adv.* **2013**, *3*, 12117−12123.
(85) Mannebach, E. M.; Spalenka, J. W.; Johnson, P. S.; Cai, Z.; Himpsel, F. J.; Evans, P. G. High Hole Mobility and Thickness-Dependent Crystal Structure in *α,ω*-Dihexylsexithiophene Single-Monolayer Field-Effect Transistors. *Adv. Funct. Mater.* **2013**, *23*, 554−564.
(86) Defaux, M.; Gholamrezaie, F.; Wang, J.; Kreyes, A.; Ziener, U.; Anokhin, D. V.; Ivanov, D. A.; Moser, A.; Neuhold, A.; Salzmann, I.; Resel, R.; de Leeuw, D. M.; Meskers, S. C. J.; Moeller, M.; Mourran, A. Solution-Processable Septithiophene Monolayer Transistor. *Adv. Mater.* **2012**, *24*, 973−978.
(87) Wedl, B.; Resel, R.; Leising, G.; Kunert, B.; Salzmann, I.; Oehzelt, M.; Koch, N.; Vollmer, A.; Duhm, S.; Werzer, O.; Gbabode, G.; Sferrazza, M.; Geerts, Y. Crystallisation Kinetics in Thin Films of Dihexyl-terthiophene: The Appearance of Polymorphic Phases. *RSC Adv.* **2012**, *2*, 4404−4414.
(88) Zhang, L.; Tan, L.; Hu, W.; Wang, Z. Synthesis, Packing Arrangement and Transistor Performance of Dimers of Dithienothiophenes. *J. Mater. Chem.* **2009**, *19*, 8216−8222.
(89) Fitzner, R.; Elschner, C.; Weil, M.; Uhrich, C.; Körner, C.; Riede, M.; Leo, K.; Pfeiffer, M.; Reinold, E.; Menaosteritz, E.; Bäuerle, P. Interrelation between Crystal Packing and Small-Molecule Organic Solar Cell Performance. *Adv. Mater.* **2012**, *24*, 675−680.
(90) Yuan, Q.; Mannsfeld, S. C. B.; Tang, M. L.; Roberts, M.; Toney, M. F.; DeLongchamp, D. M.; Bao, Z. Microstructure of Oligofluorene Asymmetric Derivatives in Organic Thin Film Transistors. *Chem. Mater.* **2008**, *20*, 2763−2772.
(91) Yuan, Q.; Mannsfeld, S. C. B.; Tang, M. L.; Toney, M. F.; Lüning, J.; Bao, Z. Thin Film Structure of Tetraceno[2,3-*b*]thiophene Characterized by Grazing Incidence X-ray Scattering and Near-Edge X-ray Absorption Fine Structure Analysis. *J. Am. Chem. Soc.* **2008**, *130*, 3502−3508.
(92) DeLongchamp, D.M.; Kline, R.J.; Lin, E.K.; Fischer, D.A.; Richter, L.J.; Lucas, L.A.; Heeney, M.; McCulloch, I.; Northrup, J. E. High Carrier Mobility Polythiophene Thin Films: Structure Determination by Experiment and Theory. *Adv. Mater.* **2007**, *19*, 833−837.
(93) Rivnay, J.; Mannsfeld, S. C. B.; Miller, C. E.; Salleo, A.; Toney, M. F. Quantitative Determination of Organic Semiconductor Microstructure from the Molecular to Device Scale. *Chem. Rev.* **2012**, *112*, 5488−5519.
(94) Schuettfort, T.; Watts, B.; Thomsen, L.; Lee, M.; Sirringhaus, H.; McNeill, C. R. Microstructure of Polycrystalline PBTTT Films: Domain Mapping and Structure Formation. *ACS Nano* **2012**, *6*, 1849−1864.
(95) Servet, B.; Ries, S.; Trotel, M.; Patrick, A.; Horowitz, G.; Garnier, F. X-ray Determination of the Crystal Structure and Orientation of Vacuum Evaporated Sexithiophene Films. *Adv. Mater.* **1993**, *5*, 461−464.
(96) Mannsfeld, S. C. B.; Tang, M. L.; Bao, Z. Thin Film Structure of Triisopropylsilylethynyl-Functionalized Pentacene and Tetraceno[2,3-b]thiophene from Grazing Incidence X-Ray Diffraction. *Adv. Mater.* **2011**, *23*, 127−131.
(97) Collins, B. A.; Cochran, J.E.; Yan, H.; Gann, E.; Hub, C.; Fink, R.; Wang, C.; Schuettfort, T.; McNeill, C.R.; Chabinyc, M.L.; Ade, H. Polarized X-Ray Scattering Reveals Non-crystalline Orientational Ordering in Organic Films. *Nat. Mater.* **2012**, *11*, 536−543.
(98) Rivnay, J.; Jimison, L. H.; Northrup, J. E.; Toney, M. F.; Noriega, R.; Lu, S. F.; Marks, T. J.; Facchetti, A.; Salleo, A. Large Modulation of Carrier Transport by Grain-boundary Molecular Packing and Microstructure in Organic Thin Films. *Nat. Mater.* **2009**, *8*, 952−958.
(99) Pingel, P.; Zen, A.; Neher, D.; Lieberwirth, I.; Wenger, G.; Allard, S.; Scherf, U. Unexpectedly High Field-effect Mobility of a Soluble, Low Molecular Weight Oligoquaterthiophene Fraction with Low Polydispersity. *Appl. Phys. A: Mater. Sci. Process.* **2009**, *95*, 67−72.
(100) Gentili, D.; Di Maria, F.; Liscio, F.; Ferlauto, L.; Leonardi, F.; Maini, L.; Gazzano, M.; Milita, S.; Barbarella, G.; Gavallini, M. Targeting Ordered Oligothiophene Fibers with Enhanced Functional Properties by Interplay of Self-assembly and Wet Lithography. *J. Mater. Chem.* **2012**, *22*, 20852−20856.
(101) Haid, S.; Mishra, A.; Weil, M.; Uhrich, C.; Pfeiffer, M.; Bäuerle, P. Synthesis and Structure−Property Correlations of Dicyanovinyl-Substituted Oligoselenophenes and their Application in Organic Solar Cells. *Adv. Funct. Mater* **2012**, *22*, 4322−4333.
(102) Liu, Y.; Yang, Y.; Chen, C.; Chen, Q.; Dou, L.; Hong, Z.; Li, G.; Yang, Y. Solution-Processed Small Molecules Using Different Electron Linkers for High-Performance Solar Cells. *Adv. Mater.* **2013**, *25*, 4657−4662.
(103) Li, Z.; He, G.; Wan, X.; Liu, Y.; Zhou, J.; Long, G.; Zuo, Y.; Zhang, M.; Chen, Y. Solution Processable Rhodanine-Based Small Molecule Organic Photovoltaic Cells with a Power Conversion Efficiency of 6.1%. *Adv. Energy. Mater.* **2012**, *2*, 74−77.
(104) Long, G.; Wan, X.; Kan, B.; Liu, Y.; He, G.; Li, Z.; Zhang, Y.; Zhang, Y.; Zhang, Q.; Zhang, M.; Chen, Y. Investigation of Quinquethiophene Derivatives with Different End Groups for High Open Circuit Voltage Solar Cells. *Adv. Energy. Mater.* **2013**, *3*, 639−646.
(105) Di Maria, F.; Gazzano, M.; Zanelli, A.; Gigli, G.; Loiudice, A.; Rizzo, A.; Biasiucci, M.; Salatelli, E.; D'Angelo, P.; Barbarella, G. Synthesis and Photovoltaic Properties of Regioregular Head-to-Head Substituted Thiophene Hexadecamers. *Macromolecules* **2012**, *45*, 8284−8291.
(106) Risk, C.; McGehee, M. D.; Brédas, J.-L. A Quantum-chemical Perspective into Low Optical-gap Polymers for Highly-efficient Organic Solar Cells. *Chem. Sci.* **2011**, *2*, 1200−1218.
(107) Zade, S. S.; Zamoshchik, N.; Bendikov, M. From Short Conjugated Oligomers to Conjugated Polymers. Lessons from Studies on Long Conjugated Oligomers. *Acc. Chem. Res.* **2011**, *44*, 14−24.
(108) Sears, J.S.; Chance, R. R.; Brédas, J.-L. Torsion Potential in Polydiacetylene: Accurate Computations on Oligomers Extrapolated to the Polymer Limit. *J. Am. Chem. Soc.* **2010**, *132*, 13313−13319.